

1 **Deltaic Sedimentary Environments in the Niger Delta, Nigeria**

2 Chinotu Franklin GEORGE ^a; David I. M. MACDONALD^a and Matteo SPAGNOLO^a

3

4 (Corresponding author: Chinotu Franklin GEORGE)

5 ^a University of Aberdeen, School of Geosciences, King's College, AB24 3UE, Aberdeen, United Kingdom.

6 Email: chinotu.george@outlook.com

7 Phone: +2348035511489, +447978354066

8

9 **Abstract**

10 This study is focused on the geomorphology of surface sedimentary environments contained in the fluvial, tidal
11 and wave-dominated areas of the Niger Delta. GIS techniques applied to high-quality Landsat and SPOT images
12 were used to identify and map landforms and processes, as well as quantitatively characterise their metrics and
13 spatial distribution. A detailed analysis shows that the extent of the Niger Delta is 70,000 km², contrary to
14 previous publications that reported 75,000 km². The delta has also been remapped and classified into mega
15 sedimentary environments: the upper deltaic plain is 69% of the total extent, while the lower deltaic plain and
16 delta front are 25% and 6% respectively. Other subunits were distinguished and mapped within the upper deltaic
17 plain such as fluvial channels, point bars, braid bars, oxbow lakes, and other lakes. Tidal channels, beaches and
18 spits were identified in the lower deltaic plain and delta front. The geometries of these sedimentary bodies
19 (landforms) appear to be relatively scale-invariant, thus meaning that from the measurement of some
20 dimensional parameters (e.g. the length) it is possible to estimate all others (e.g. the width and overall extent).
21 This is an aspect of great relevance in subsurface analyses where it is often difficult to predict the extent of
22 sedimentary bodies. The correlation between channel width and length ($r^2=0.9$), is the strongest relationship
23 found between sedimentary body metrics.

24

25 **Keywords:** Sedimentary environments, Niger Delta, geomorphic units, landforms, recent sand body geometries,
26 deltaic analogues.

27

28 **1 Introduction**

29 The Niger Delta is located in southern Nigeria in West Africa; it has been a research focus for the last few
30 decades because it is a prolific oil and gas province. It is one of the largest regressive deltas in the world with an
31 area (onshore and offshore) of 300,000 km² (Kulke, 1995). The Niger Delta is the sixth largest oil producing
32 delta (Reijers, 1996), and top 20 oil producing region, in the world. The pioneering studies by NEDECO (1954,
33 1959, 1961), Hill and Webb (1958), Allen and Wells (1962), Allen (1963, 1965, 1970) and Oomkens (1974)
34 have described the sedimentology, morphology, and physiography of the Niger Delta.

35

36 Allen (1965, 1970) used aerial photographs to delineate the lateral extent of the entire Niger Delta and its
37 various sedimentary environments (also referred to as deposits, geobodies, and landforms in this paper) as
38 shown in Figures 1 and 2. However, Allen's and other works (NEDECO, 1954, 1959, 1961; Allen, 1965, 1970;
39 Oomkens, 1974) did not cover the quantitative and statistical aspects of the facies architecture and dimensions.
40 So, the near-surface geology and the plan dimensional characteristic of the landforms in the Niger Delta are still

41 not fully studied, whereas this type of study has greatly advanced our understanding of other deltas around the
42 world in recent years. In the Rhine-Meuse, for example, studies have included an estimate of the Holocene
43 sediment budget, the paleogeographic reconstruction, the general geomorphology, the fluvial response to
44 Paleocene climate change and an analysis of river channel and bar patterns (Erkens et al., 2006; Berendsen et al.
45 2007; Uehlinger et al., 2009; van Balen et al., 2010; Kleinhans et al., 2011). In the Mekong River delta, the Late
46 Holocene evolution of the Mekong subaqueous delta was studied by Xue et al. (2010) as well as the
47 geomorphological characterisation of the mixed bedrock-alluvial multi-channel network by Meshkova &
48 Carling (2012). The Danube Delta is another well-studied area; its analysis demonstrated that it has multiple
49 growth lobes, as the interplay between the delta-forming processes is varied in space (Bhattacharya and Giosan,
50 2003; Giosan et al. 2006; Giosan and Goodbred, 2007). Morphodynamic studies of deltas have also been carried
51 out in the Indus (Giosan et al., 2006) and Mississippi deltas (Parker and Sequeiros, 2006). Studies of the
52 Brahmaputra and Amazon deltas and others are documented in Sambrook-Smith et al., (2005), while the
53 Mississippi, Missouri and Columbia rivers are the focus of Fisk (1947), Komar (1984), Blum and Roberts
54 (2009), Edmonds and Slingerlands (2009). Other studies on deltas can be found in Woodrofe (2000), Ashton
55 and Giosan (2007) and Hoyal and Sheets (2009).

56

57 The map of sedimentary environments in the Niger Delta has not been updated since the work of Allen (1965)
58 and Short and Stauble (1967), both based on aerial photos. In this study, the sedimentary environments have
59 been completely re-mapped, by using high-quality Landsat TM and SPOT colour satellite images. We have
60 applied GIS technique to recent satellite images of the Niger Delta to identify and classify geomorphic units
61 across a range of scale, within distinct mega sedimentary environments. As part of this exercise, the geometric
62 dimension of each geomorphic unit were measured, and statistical equations and mathematical relationships
63 were derived. In addition, the spatial extent and distribution of these geomorphic units have been analysed,
64 which has given new information into the landforms and the processes that created them. Collectively, this
65 information provides insights on similar environments that are now buried deep beneath the surface both in the
66 Niger Delta and other deltas. This is of significant value to the petroleum industry; in reservoir characterization
67 and modelling, analogues are fundamental to study and calibrate subsurface reservoir facies elements (Borer and
68 Harris, 1991; Tyler and Finley, 1991; Grant et al., 1994; Sarg et al., 1999; White and Barton, 1999; Willis and
69 Gabel, 2001; Wood, 2004, Jin et al. 2017; Pierik et al. 2017; Zimmermann et al. 2018).

70

71 **2 Geology of the Niger Delta**

72 The Niger Delta is in the southern part of Nigeria, between longitudes 3-9° E and latitudes 4°31'-5°20'N and lies
73 in the humid tropics (Short and Stauble, 1967; Allen 1970; Asseez, 1989). The western border is the Benin
74 Flank and the eastern is the Calabar Flank (the flanks are regional rift faults); the southern coastal margin is
75 open to the Atlantic Ocean (Asseez, 1989). The Niger Delta basin began to form in the Cretaceous when the
76 African plate separated from the South American plate; the basin is bounded by rift faults on its northwestern
77 and northeastern edges (Burke and Whiteman, 1973; Burke and Dewey, 1974; Olade, 1975; Whiteman, 1982;
78 Fairhead and Blink, 1991; Guiraud and Maurin, 1991; 1993). The regressive clastic sequence in the Niger Delta
79 started building in the Paleocene and has since then built sediments that now reach a thickness of 12,000 meters
80 (Evamy et al, 1978). These sediments are deposited into six diachronous depo-belts i.e. sediments are younger

81 towards the Atlantic Ocean in the south. The depobelts are: (i) Northern Delta, (ii) Greater Ughelli, (iii) Central
82 Swamp I, (iv) Central Swamp II, (v) Coastal Swamp and (vi) Offshore, each separated from the other by
83 regional faults (Doust and Omatsola, 1990). The depobelts were by Tuttle et. al. (1999), who created a map that
84 shows the ages of the depobelts, from northern Niger Delta to the sea, using paleo-coastlines as boundaries on
85 plan-view and the regional faults on the section-view. The coastline has prograded seaward in discrete
86 successive stages for over 35 Ma (Tuttle et. al. 1999). A similar depobelt classification of the Niger Delta,
87 looking at the plan-view only was done by Oomkens (1974) and Allen (1963, 1965a), and it was focused on
88 Holocene (Quaternary) surface and near-surface sediments.

89

90 The sedimentary pile of the Niger Delta has been grouped into three stratigraphic units: the continental, paralic
91 and marine sequences based on the sand/shale ratio (Short and Stauble, 1967; Avbovbo, 1978). Evamy et al.
92 (1978) named these stratigraphic units the Akata, Agbada and Benin formations respectively from bottom to top.
93 The Agbada Formation is the target formation in the exploration of oil and gas. It is about 3000 meters thick and
94 ranges from the Paleocene to Recent. In the Agbada Formation, the shale intercalation forms the seal while
95 growth faults, associated roll-over anticlines, and antithetic faults are the main traps that enhance petroleum
96 accumulation (Asseez, 1989). The delta appears to be in near isostatic equilibrium and has grown in thickness
97 and volume in the absence of tectonic control (Stoneley, 1965).

98

99 **3 Data and Methodology: GIS data and digitized maps**

100 The raster Landsat TM and SPOT satellite imagery is the key dataset used to map all recognisable sedimentary
101 environments, which include the mega-environments: upper delta plain, lower delta plain, and the delta front,
102 each dominated with fluvial, tidal and wave-related deposits, respectively (see Figure 1). Within these mega
103 sedimentary environments, various subunits/environments are distinguishable based on their morphology and
104 following Bridge (2003). These include: distributary fluvial channels, tidal channels, braid bars, point bars,
105 oxbow lakes, crevasse splays, cut-off channels, other lakes and ponds, beaches, and spit. Landforms were
106 recognised and digitised from Landsat and SPOT satellite images using bands 5, 4 and 3 (RGB) and 4, 3 and 2
107 (RGB) respectively. The resolution of the satellite images, 20 m for Spot and 28.5 m for Landsat TM, was high
108 enough to resolve all studied landform. The mapping and identification of the various units and subunits were
109 based on pattern recognition considering elements of interpretation such as: tone, textures, shape, and pattern
110 amongst other elements, and most importantly, the natural association of these landforms. For example,
111 channels were identified because of their reflectance (water-filled part), tone and shape, all of which are clearly
112 different from the adjacent environments (e.g. floodplain). Other elements have proved to be more difficult to
113 map. For example, while the boundary between point bars and channels can be easily identified, that between
114 point bars and the floodplain is not always clear. While the former can be traced following the reflectance
115 contrast between water and sand, the latter requires the identification of the termination of the scroll-swale,
116 which is often water-logged. Accurate geo-referenced maps of the Niger Delta were created (Figures 1 and 2).
117 The size (width and length), aspect ratio, shape, orientation, connectivity and continuity of the identified
118 sedimentary environments were analysed in a GIS environment by using ArcGIS and the Hawth's Analysis
119 tools (<http://www.spatial ecology.com/htools/overview.php>).

120

121 **4 Results and Discussion**

122

123 **4.1 Extent of Niger Delta**

124 There are inconsistencies in the reported area of the Niger Delta as published by Kravtsova et al. (2008); with
125 eight different values reported ranging from 1,140,000 km² to 2,240,000 km². Some of these values are
126 unrealistic and it is not clear if these include the submerged part of Niger Delta or not. As a result, the area
127 derived from this paper is only compared with the work of Allen (1970) and Short and Stauble (1967); both of
128 which have been quoted most frequently in publications. This study revealed that the terrestrial portion of the
129 Niger Delta covers an area of 70,000 km², and with an axial distance of 221 km. The axial distance is measured
130 from the landward tip at Onitsha to the coastline at the Sombreiro-Nun rivers (the farthest seaward protrusion of
131 the coastline). The coastline is 650 km long; from the Rio-del River (east) to the Lagos Peninsula (west)
132 (Figures 1 and 2). These figures (Figures 1 and 2) are very important as they serve as a reference in estimating
133 dimension and areal extent of subsurface sandbodies. They are also important in estimating the rate of growth of
134 the delta seaward or the impact of destructive processes, such as erosion, over time.

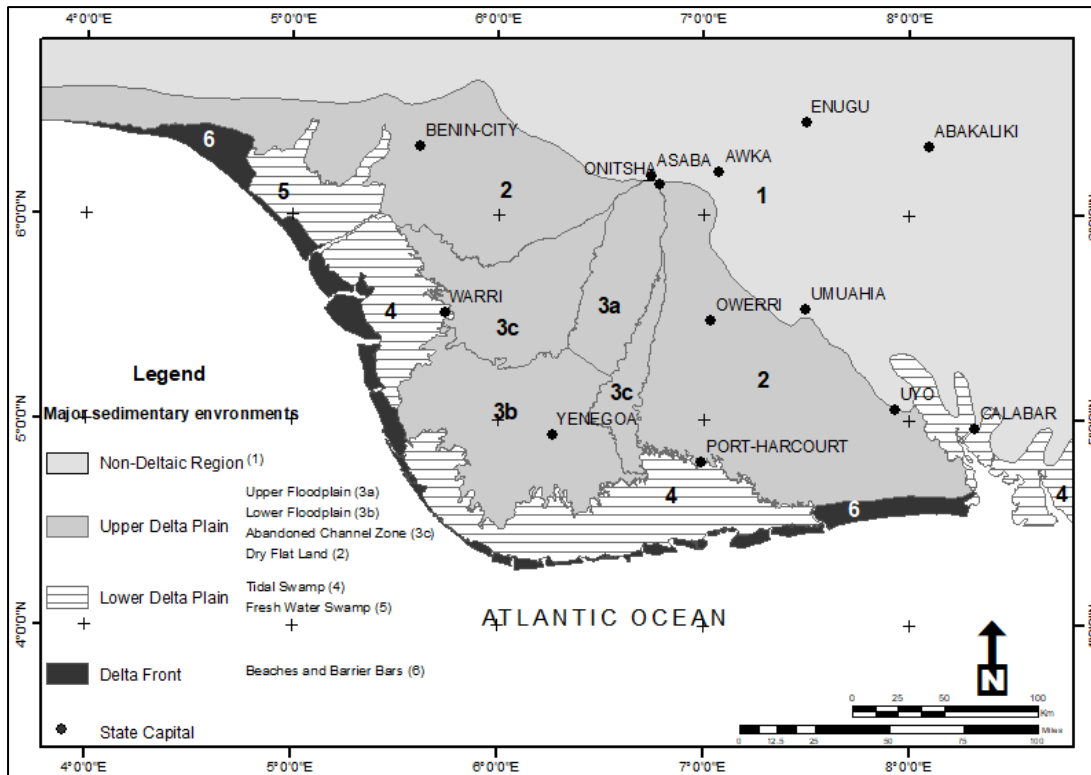
135

136 The area (70,000 km²) of the Niger Delta is 5,000 km² less than the areal extent previously estimated by Allen
137 (1970) and Short and Stauble (1967). The axial distance measured by Doust and Omatsola (1990) was 300 km,
138 which is about 80 km more than the current result. The outer boundary of the Niger Delta, as defined by Short
139 and Stauble (1967), was digitised and compared with that from this study. The differences between the extent of
140 the Niger Delta in this study and the previous works could not possibly be related to coastal erosion since the
141 Niger Delta is generally a prograding delta. The reduction in the area of the Niger Delta by six percent and in
142 the axial length by 26 percent are possibly related to the different techniques used. Allen (1970) and Doust and
143 Omatsola (1990) used aerial photographs, which are prone to errors due to mosaic “stitching” parallax effects
144 (Curran, 1983). In this study, Landsat TM and SPOT images, which have a higher resolution and little or no
145 distortion, were used, coupled with detailed algorithms and processing software (ArcGIS) which was used in the
146 image interpretation and analysis of the areal extent.

147

148 **4.2 Mega-sedimentary environments in the Niger Delta**

149 The upper delta plain is the largest environment covering 69% of the entire Niger Delta, while the lower delta
150 plain and the delta front cover 25% and 6% respectively (Figure 1). These zones (the upper delta plain, lower
151 delta plain, and the delta front) are the three main mega-sedimentary environments in the subaerial and
152 subaqueous Niger Delta (Allen, 1965, 1967, 1970; Short and Stauble, 1967; Doust and Omatsola, 1990).

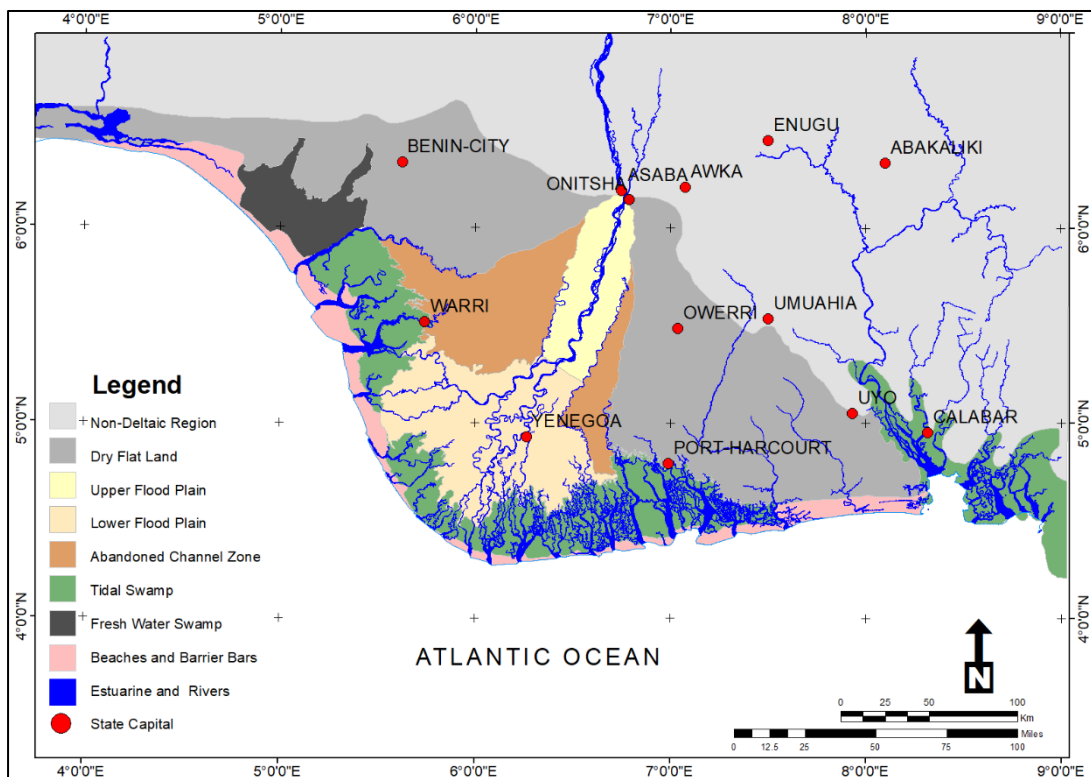


153

154 Figure 1: Map of major sedimentary environments in the Niger Delta; showing upper delta plain (continental),
 155 lower delta plain (transition) and the delta front (marine).

156

157



158

159 Figure 2: Map of Niger Delta showing major sedimentary environments.

160

161

162

163 **4.3 Upper delta plain**

164 The dry flat land, upper floodplain, lower floodplain and abandoned channels zone (floodplain transition zone)
165 are all parts of the upper delta plain (Figures 1 and 2). In the upper delta plain, the abandoned channel zone
166 (floodplain transition zone) is between the upper floodplain and the dry flat land. The Niger River runs through
167 the upper delta plain and divides it into two approximately equal parts: the eastern part and the slightly larger
168 western part (the area of the subunits will be reported in Sections 4.3.1, 4.3.2, 4.3.3 and 4.3.4).

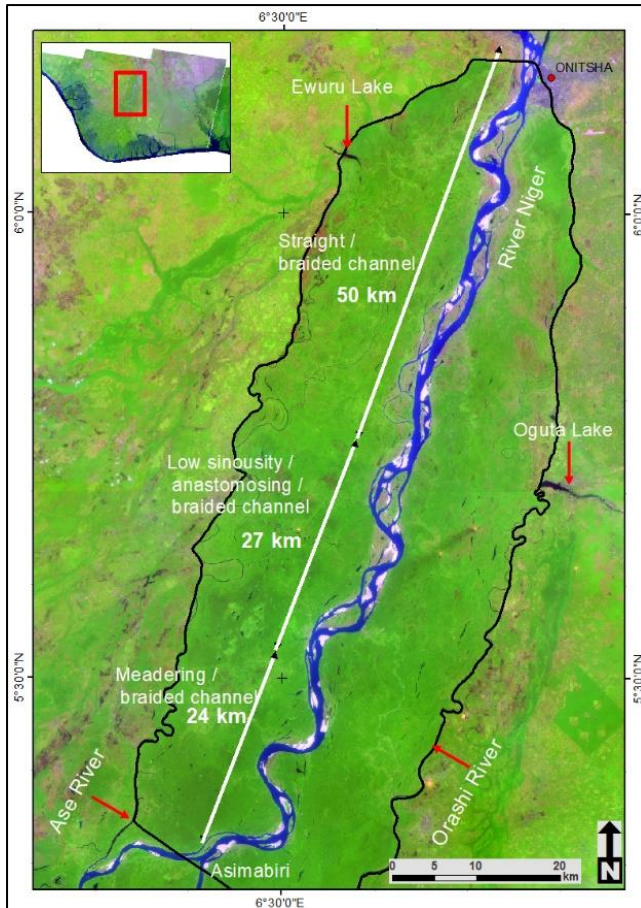
169
170 **4.3.1 Dry flat land**

171 The dry flat land is the largest of the subunits in the upper delta plain, with an area of 27,413 km² and covering
172 61% of the upper delta plain. It borders the boundary between the Niger Delta and the hinterland (Figures 1 and
173 2) and is annexed to the upper delta plain since it is part of the Benin Formation (Short and Stauble, 1967).
174 There are no obvious water-filled channels in the dry flat land within the resolution of the satellite image used.
175 Therefore, the dry flat land is relatively stable and not impacted upon by recent deposition or erosion caused by
176 rivers and tide. However, it is possible that ephemeral channels drain the dry flat land.

177
178 **4.3.2 Upper floodplain geometry**

179 A floodplain is the strip of land or a flat or smooth area adjacent to river channel which is normally covered
180 during seasonal floods and subjected to sedimentation when the river overflows its banks (Miall, 1992; Bridge,
181 2003). In the Niger Delta, the upper floodplain is swampy and has a forest of tropical trees (Whiteman 1982).
182 The upper floodplain of the Niger River starts from Onitsha (its apex, as shown in Figure 1) at the entry point of
183 the river into the Niger Delta basin (see also Whiteman 1982). It is clearly demarcated from the abandoned
184 channel zone by two rivers: the Orashi River in the east and the Ase River in the west (Figure 3).

185
186 The area of the upper floodplain is 3,166 km² with a length of 105 km, measured from Onitsha to the first point
187 of its bifurcation at Asimabiri (Figure 3). The average width on either side of the Niger River is 31 km, though
188 the western side can be 1 to 5 km wider than the eastern side. The ratio of the width of the upper floodplain to
189 the width of the Niger River channel ranges from 4 to 19 (mode and average are 15) and increases downstream.
190 Although, this ratio fluctuates along the course of the river, the average value does have a good statistical
191 relationship, which can be used to predict the size of one of these elements when the other is known. Apart from
192 channel width, it is likely that a combination of the volume of water released into the floodplain during river
193 overflow, the topography, vegetation, climate, and hydrology constrain the geographic extent of the floodplain
194 (Fagan and Nanson, 2004). The outer margins of the upper floodplain (at the boundary with the abandoned
195 channel zones) are bordered by the rivers Ase and Orashi (Figure 3), which can also constrain the extent of the
196 floodplain as they serve as conduits that can redirect water flow (also see Allen, 1965).

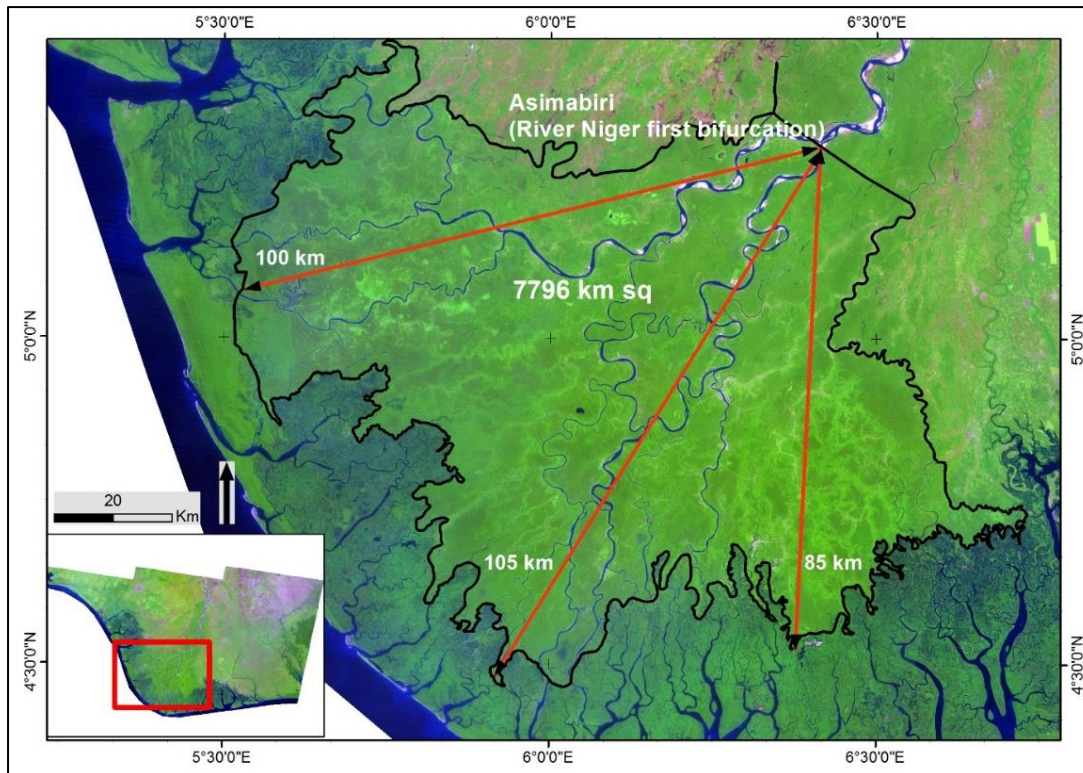


197

198 Figure 3: A satellite image of the upper floodplain showing the channel style of River Niger from the apex to the
 199 first point of bifurcation at Asimabiri. The entire length of River Niger is braided, changing from straight
 200 channel at the apex to meandering channel at the lower channel section.
 201

202 **4.3.3 Lower floodplain geometry**

203 The upper limit of the lower floodplain is at Asimabiri, the first bifurcation point of the Niger River within the
 204 delta, which is also its boundary with the upper floodplain (Figures 1 and 4). The seaward boundary interfingers
 205 with the lower delta plain and, in some parts, with the beaches. The River Niger bifurcates first into two major
 206 distributary rivers (4th order rivulets): the Forcados and the Escravos, then further into other rivers up to 1st order
 207 rivulets from the main 5th order terminal distributary channels (Olariu and Bhattacharya, 2006) (Figures 3 and 4)
 208 (stream ordering after Strahler, 1957). Other sub-environments found in this zone include: distributary fluvial
 209 channels, crevasse splay, point bars, ox-bow lakes, ponds, and cut-off channels.



210
 211 Figure 4: Map of the lower floodplain of River Niger, showing the maximum length in the three growth lobes
 212

213 The lower floodplain fans out seawards from a minimum width of 30 km, at the upper boundary, to a maximum
 214 width of 140 km, downstream at the lower boundary with the lower delta plain; it covers an area of 7,796 km².
 215 The lower floodplain has three distinct growth lobes which reflect the dominance of sediment progradation from
 216 the feeder fluvial channels (Figure 4). The progradation is more at the center (105 km in length), and less in the
 217 east (85 km) and western (100 km) portions.

218
 219 **4.3.4. Abandoned channel zone**

220 The zone of abandoned channels, or the floodplain transition zone, is a region between the dry land and the
 221 upper floodplain (as shown in Figures 1 and 2). The Ase and Orashi rivers are the boundaries between the
 222 abandoned channel zones and the upper floodplain on the west and east respectively.

223
 224 The western zone of the floodplain transition covers an area of 4,902 km², which is about three times the area
 225 covered by the eastern side (1,565 km²). The elevation of the abandoned channel zone is slightly higher than the
 226 lower delta plain. It is possible that this topographic difference at the southern boundary of the abandoned zones
 227 roughly coincided with ancient coastline at some point in the development of the delta. Therefore, the
 228 abandoned zone could have been formed under a unique set of delta-forming conditions (preferentially fluvial
 229 dominated, given the abundance of fluvial channel traces). The sediments at that time could have prograded
 230 more toward the west, causing the western zone to grow more than its eastern counterpart. The traceable
 231 channels on these zones run north-south and radiate from the apex of the Niger Delta like the present-day Niger
 232 River. Given their convergent geometry, it is likely that the abandoned channels in both zones (east and west)

233 were originally connected to the Niger River but later disconnected due to channel or delta switching. It is less
234 likely that these channels formed in-situ as is common in semi-arid regions (Fagan and Nanson, 2004).

235

236 The abandoned channels are not filled with water, but they can be ephemeral and key in draining these regions
237 during and after flooding. Bridge (2003) described similar features as “drainage channels”. It is possible that, in
238 the geologic past, these abandoned channels were major conduits through which sediments were supplied to the
239 Niger Delta’s coastal margin. Now sediment supply through these abandoned channels is discontinued. This
240 implies that the tidal channels they are supposed to connect and feed sediment to are now starved of sediment
241 supply. So, those tidal channels, which are either side of the Niger Delta coastal margin, have fewer sediments
242 deposited in them, as reported by Doust and Omatsola (1990). As a result, the tidal channels in the tidal-process
243 dominated western flank (Figure 18a; e.g. Benin, Escravos and Forcados channels) and eastern flank (Figure
244 18b; e.g. Bonny, New Calabar, and Sombreiro channels) are wider than in the central flanks, where sediment
245 supply is continuous and connected to active fluvial channel.

246

247 The abandoned channels can contain water in the form of lakes or ponds for a considerable length of time after
248 becoming inactive and before eventually being completely silted up or filled with clay deposits (Nichols, 1999;
249 Miall, 1992). The transition zone hosts other sub-units like: cut-off channels, crevasse splay, over-bank deposits,
250 ponds, and lakes. Activities such as farming have left these zones on either side of the Niger River with little
251 natural vegetation.

252

253 **4.4 Lower delta plain and delta front**

254 The lower deltaic plain and the delta front are mega-sedimentary environments of the Niger Delta, within which
255 tidal swamp, tidal flats, beaches, spits, and estuaries are contained, as shown in Figures 1, 2, and 3. The lower
256 deltaic plain is separated from the upper deltaic plain by a bayline (Bhattacharya 2006 and 2010). The bayline is
257 marked by the boundary defining estuarine (tidal channels) termination, beyond which tidal incursion is
258 insignificant. The entire delta front is rimmed with elongate beaches and barrier islands typical of wave-influenced
259 delta fronts (Olariu and Bhattacharya 2006; Ainsworth et al 2011). Tidal channels are ubiquitous in these regions;
260 these cut through the delta front, dividing it into blocks of beaches-barrier islands. The areal extent of the lower
261 deltaic plain is 16,625 km² which is 25% of the entire area of the Niger Delta while the delta front covers
262 4,138 km² and is 6% (Figures 1, 2 and 3). The areas of the lower deltaic plain and the delta front together are
263 20,763 km².

264

265 Oomkens (1974), who studied the Quaternary (Holocene) Niger Delta, reported that the area of lower delta plain
266 is about 5,000 km² which is considerably less than the area recognized in this work. Also, Allen (1970) reported
267 that the area of the tidal swamp (lower deltaic plain) is 9,000 km², which is about half of that from this study. The
268 method or technique used by Oomkens (1974) and Allen (1970) respectively to estimate the areas were not clearly
269 stated in their papers. Therefore, result from this work is considered more reliable as it is extracted from high-
270 quality satellite images with ArcGIS.

271

272 **4.4.1 Tidal (Mangrove) swamp environment**

273 The mangrove swamps have been formed wherever the tide pushes saltwater inland through the tidal and
274 transverse channels and creeks. Mangrove swamps extend 480 km on the southern margin parallel to the coast
275 (Figure 1). In the axial parts of the delta, the swamp belt is mostly 8-16 kilometres across, merging with the lower
276 floodplain at the northern boundary (Allen, 1965a). Swamp width, measured in North-South direction, increases
277 to 30-40 km on the delta flanks. In the marginal estuaries of the Calabar and Rio del Rey, east of the delta, the
278 swamps are sparse, terminate at the sea and pinch out landward.

279

280 **4.5 Geometries of landforms associated with the upper deltaic plain**

281 In the upper delta plain landforms include: fluvial river channels, point bars, braid bars, lakes, ponds, and ox-
282 bow lakes. These sand bodies play a significant role in the storage of oil and gas when preserved in the
283 subsurface. In the following subsections, the geometries and reservoir implications are discussed.

284

285 **4.5.1 Channel geometries of the Niger River**

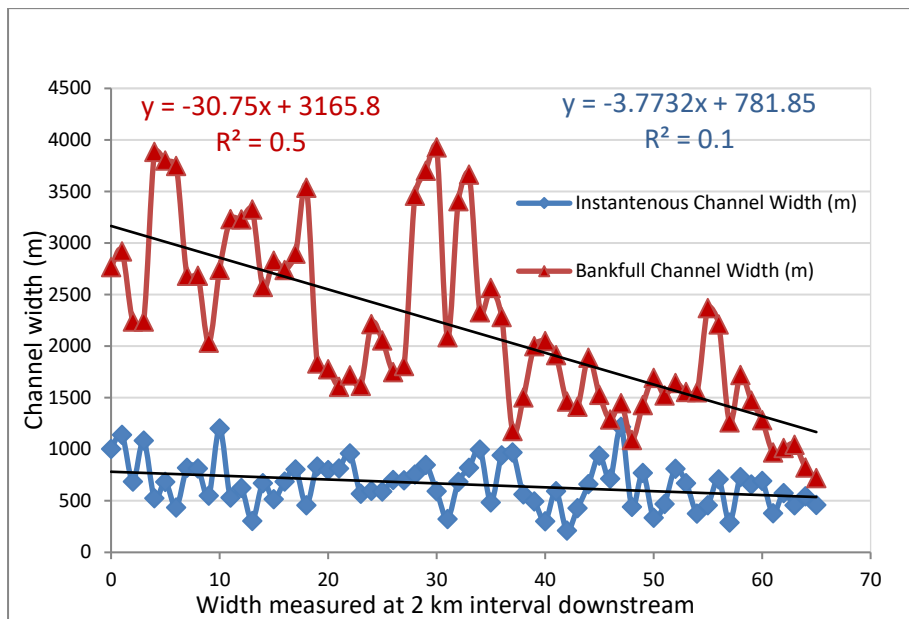
286 The section of Niger River from proximal to distal covers variable segments which include: low sinuosity
287 (Sinuosity Index, S.I. less than 1.5) straight and braided channels (50 km) ; low sinuosity anastomosing channels
288 and braided rivers section (27 km); high sinuosity meandering channels and braided section (24 km) (Figure 3).
289 This morphological classification is typical of many other river systems (Ferguson, 1987; Nanson and Knighton,
290 1996; Schumm et al., 2000; Schumm, 2005; Kleinhans and Van den Berg, 2011). The Niger River is a
291 distributive channel system and has typical dendritic channels (Howard, 1967), which are controlled by
292 topography, hydrodynamics, and geology. The entire length of the River Niger is characterised by the presence
293 of braid bars, indicative of high sediment discharge (Bridge 2003, p. 154); their abundance progressively
294 reduces downstream.

295

296 **4.5.2 Channel width variation downstream**

297 The length of the Niger River from Onitsha to the coast on the Forcados arm is 327 km and nearly the same
298 (321 km) on the Nun River arm. Like other rivers (Kleinhans, 2010; Kemp, 2004; Luchi et al, 2010; White et al,
299 2010; Davidson et al, 2011), the Niger River channel width decreases from the apex to the coast linearly,
300 ranging from 4000 m to 200 m (1500m is the mode), while its depth increases, thus keeping the volume of water
301 fairly constant (Olariu and Bhattacharya 2006). The Niger River width generally decreases linearly by 30 m
302 every 2000 m moving downstream (Figures 4 and 5). However, after points of bifurcation, the reduction in
303 channel width is drastic with significant impact on the overall channel width gradient (Edmonds and
304 Slingerland, 2007, 2008, 2009). For example, there is a significant step-down in the width of the Niger River
305 after the first bifurcation at Asimabiri, beyond which the Braiding Index (sensu Friend and Sinha, 1993) also
306 reduces drastically, implying a low gradient. Braiding Index BI is the braid channel ratio (L_{ctot}/L_{cmax}). L_{ctot} is the
307 sum of the mid-channel lengths of all the segments of primary channels in a reach and L_{cmax} is a measure of the
308 mid-channel length of the widest channel through the reach (sensu Friend and Sinha, 1993). The channel shows
309 high variability in width further downstream, which is due to the presence of braid bars. These braid bars reduce
310 channel width and their blocking effect varies along-channel flow velocity, which, and in turn, causes the
311 intensity of bank erosion and deposition to also vary. This factor is responsible for the high variability in the
312 channel width in the Niger River. Distributary channel (tidal channel) width increases geometrically

313 downstream because of tidal impact, which is highest at the coast and wanes landward. It is, in fact, a marker for
 314 distinguishing between fluvial and tidal channels in the Niger Delta.
 315



316
 317 Figure 5: Channel width variation of River Niger (from Onitsha i.e. graph origin to the first bifurcation at
 318 Asimabiri). Instantaneous channel width (blue) is the width as seen on the images interpreted, it measures the part
 319 of the channel covered by water. While bank-full channel measurement assumes that mid-channel and side-bars
 320 were submerged. So, its measurement extended beyond the water body to the thickly vegetative side of the river
 321 bank, in some areas.

322
 323 **4.5.3 Sinuosity Index of channels**

324 The Sinuosity Index (sensu Spagnolo et al., 2008) of the Niger River ranges from 1.3 to 2.9 and increases
 325 downstream. The sinuosity of Imo (east), Sombreiro (east) and Escravos (west) rivers are high, with an average
 326 and modal sinuosity above 2.0. As the discharge of the channel's flow wanes, the meanders grow larger and the
 327 sinuosity of the fluvial channel increases towards the coast (Seppala, 2013; Nichol, 1999). The sinuosity of the
 328 channels farther away from the axis of the Niger Delta to the flanks is generally higher than that of the main
 329 Niger River channel. Therefore, sinuosity not only increases downstream but also increases outward from the
 330 axis of the Niger Delta. The factors that control the spatial variation in sinuosity in the Niger Delta are not clear
 331 but there seems to be a relationship between channel length and width. The sinuosity of the channels that are
 332 long and narrow is generally higher than 2.0 (see Figures 15 and 16). There is also a progressive increase in
 333 sinuosity with stream order, particularly from fifth order to first order, in distributary channels.

334
 335 **4.5.4 Point bars**

336 Point bars form inside bends of rivers below the slip-off slope (i.e. they form by accretion inside an expanding
 337 loop or meander of a river). On the satellite image, point bars were identified in the meandering portion of the
 338 river, based on texture and pattern on the image. The vegetation within the point bar shows a lighter green
 339 reflectance as compared to the adjacent floodplain which is darker green reflectance. Also, within the mapped
 340 point bars, the scroll and swale topography are evident: at the scroll (ridge), the vegetation is dense; whereas at
 341 the swale (trough), the vegetation is sparse and sometimes the sands are exposed, showing high (if bare) or

342 darker (if water-filled) reflection. The side of the point bars in contact with the main fluvial channel is easily
343 delineated by the blue water body. In general, the topographic pattern makes it easy to identify, map, and
344 measure the scroll-swale width. The active sandy bars are separated from the vegetative part by channels; as
345 such they are not really considered as part of the point bars. Although these landforms are transient and ever-
346 changing, sometimes even merging with braid bars to form complex assemblages, characterisation of their
347 morphology has been attempted here based on what we were able to observe and measure on the satellite
348 imagery. Hopefully, this gives an overview of the range of geometries that might be of relevance, for example,
349 to analogue studies.

350
351 There are 24 point bars mapped in the Niger Delta and their geometric dimensions are presented in Table 1.
352 They are all associated with the fluvial channels and mainly within the upper delta plain covering the upper and
353 lower floodplains. Traces of other point bars associated with other ephemeral channels were also observed in the
354 upper floodplain. Four representative point bars are shown in Figure 6. The length of all mapped point bars
355 varies between 1,500 m and 10,021 m and 91% of the length is below 5000 m. The width of the point bars
356 ranges from 650 m to 5,026 m (with a mode of 2500 m). The swales–scroll width (accretion bounding surfaces)
357 ranges from 76 m to 310 m (mostly 200 m). The ratio of point bar length to width ranges from 0.5 to 3.7 and the
358 ratio of the point bar width to main channel width ranges from 1.7 to 10.6. The length, width, and area of point
359 bar, sinuosity and channel length and channel width associated with the point bar are plotted to validate the
360 dependence of a set of these parameters to one another. The plots of point bar length against area (Figures 7 and
361 8) and the point bar width against area (Figure 9) demonstrate a significant relationship. The length and width of
362 point bars correlate positively with the overall size (area), with a correlation coefficient varying from 0.8 to 0.9.
363 The summary of the relationships derived from these plots is also shown in Table 1 and in the empirical
364 equation (Equation 1).

365
366 This study shows that a ratio between 2 to 10 exists between point bar width to channel width (see Table 1 and
367 Equation 1).

368
369 $W_p = cW_{ch}$ (regardless of sinuosity)Equation 1

370 Where: W_p = point bar width
371 W_{ch} = channel Width,
372 c = a parameter that ranges from 2 to 10

373
374 The point bar width is generally about half the point bar length, except in zones of high sinuosity ($SI > 2.5$);
375 where point bar width tends to be equal to, or higher than, the point bar length (see plots in Figures 7,8 and 9).

376
377 The results of this study are similar to those from Leopold et al. (1964). Their equation is one among many
378 equations that relates point bar width with channel width at a uniform sinuosity of 1.5, with c ranging from 2 to
379 12 (Leopold and Wolman, 1960; Leopold et al, 1964). Other studies of point bars and related fluvial bodies by
380 Fielding and Crane (1987), Bryant and Flint (1993), Cuevas Gozalo and Martinius (1993), North (1996), De
381 Rooij et al, (2002) and Ghinassi et al, (2016) have shown that relationships exist between parameters such as

382 thickness, length, width, volume, river sinuosity and bend tightness. Also, and importantly, they confirm that
383 most fluvial landforms are scale invariant.

384

385 The overall geometry of point bars is not only influenced by sediment erosion and deposition along the channel
386 bank but also by bank stability, and the river hydrodynamics. In turn, bank stability depends on the geology and
387 vegetation. Braiding can also affect the formation and geometry of the point bars; as areas with high braiding
388 index have fewer point bars. However, from this study, point bars are mostly associated with meandering
389 sections of the channel (Figures 7, 8 and 9). The statistical relationship between point bar parameters and
390 channel parameters identified here (Equation 1) could be used to estimate point bar length or width when the
391 other parameter is known. This is important for the characterisation of subsurface sedimentary bodies.

392

393 Chute or cut-off channels are developed across the top of abandoned point bars as a result of flood events or
394 braiding, during which the main channel is choked with sediment. They are essential to demarcate point bars
395 from the floodplains. Apart from the chute channel associated with the Niger River, other isolated channels (or
396 ponds) are abundant in the floodplain of the Niger Delta.

397

398

399

400

401

402

403

404

405

406

407

408

409

410

411

412

413

414

415

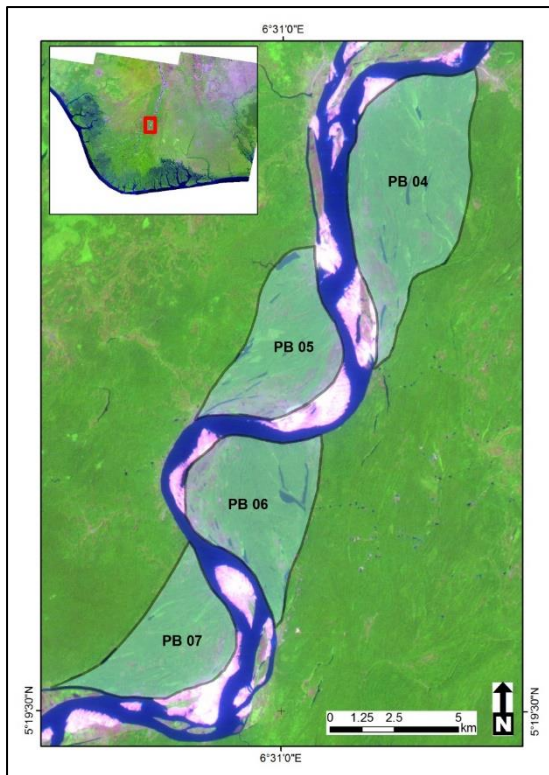
416

417 Table 1: Point bar geometric dimensions in the Niger Delta of River, Forcados and Nun arm inclusive.

Point bar geometric dimensions											
Point bar Name	Associated River	Point bar Area (km ²)	Point bar Length (m)	Point bar Width (m)	Average scroll Width (m)	Channel Length (m)	Channel Width (m)	Sinuosity Index	Point bar Length/Width	Point bar Width/Channel Width	Point bar Scroll width/Width
PB 01	River Niger	15	3270	3816	171	5244	683	1.60	0.9	5.6	22.3
PB 02	River Niger	10	2983	2299	185	4300	848	1.44	1.3	2.7	12.4
PB 03	River Niger	12	3865	3327	241	5798	812	1.50	1.2	4.1	13.8
PB 04	River Niger	36	10021	4790	310	11756	829	1.17	2.1	5.8	15.5
PB 05	River Niger	21	5232	3856	185	6972	899	1.33	1.4	4.3	20.8
PB 06	River Niger	24	4558	5026	216	7573	579	1.66	0.9	8.7	23.3
PB 07	River Niger	19	4876	3784	243	6564	615	1.35	1.3	6.2	15.6
PB 08	Forcados	5	1749	2884	163	3581	415	2.05	0.6	6.9	17.7
PB 09	Forcados	11	3702	2722	141	5191	398	1.40	1.4	6.8	19.3
PB 10	Forcados	21	4548	4398	176	6700	703	1.47	1.0	6.3	25.0
PB 11	Forcados	9	5081	1761	164	5929	532	1.17	2.9	3.3	10.7
PB 12	Forcados	1	1559	798	76	1776	276	1.14	2.0	2.9	10.5
PB 13	Forcados	2	2346	650	130	2504	346	1.07	2.9	1.9	10.5
PB 14	Forcados	1	1957	743	82	2162	416	1.10	3.0	1.8	5.0
PB 15	Nun	4	2736	1017	131	2997	406	1.10	3.7	2.5	9.0
PB 16	Nun	3	2408	3936	135	5378	372	2.23	2.4	10.6	7.7
PB 17	Nun	4	1941	2222	130	3476	385	1.79	0.5	5.8	29.2
PB 18	Nun	5	3715	729	131	3910	429	1.05	1.7	1.7	17.1
PB 19	Nun	5	2382	1879	138	3183	510	1.34	3.3	3.7	5.5
PB 20	Nun	6	2007	3489	144	4704	360	2.34	1.1	9.7	13.6
PB 21	Nun	4	1843	2410	131	3371	439	1.83	0.5	5.5	24.3
PB 22	Nun	10	2868	3257	291	4707	438	1.64	1.2	7.4	18.4
PB 23	Nun	5	1961	2820	241	3709	300	1.89	0.6	9.4	11.2
PB 24	Nun	4	1737	2637	159	3961	296	2.28	0.6	8.9	11.7

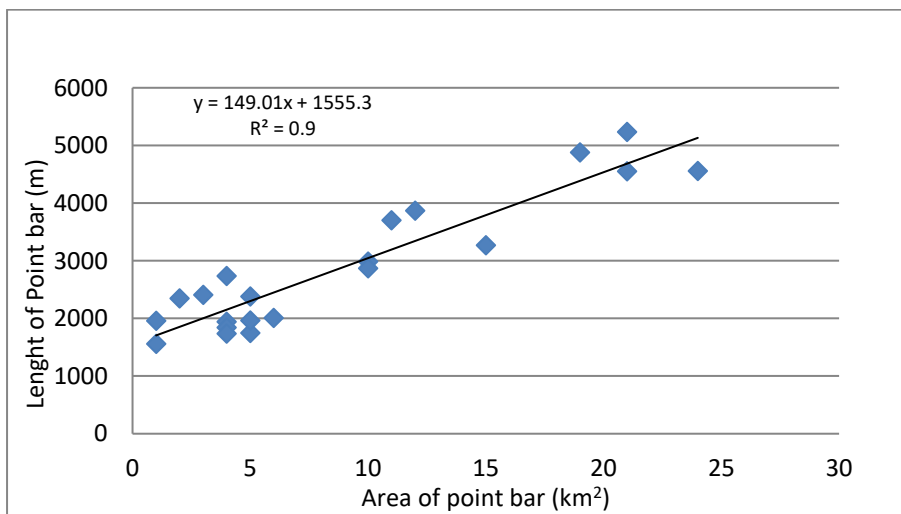
418

419



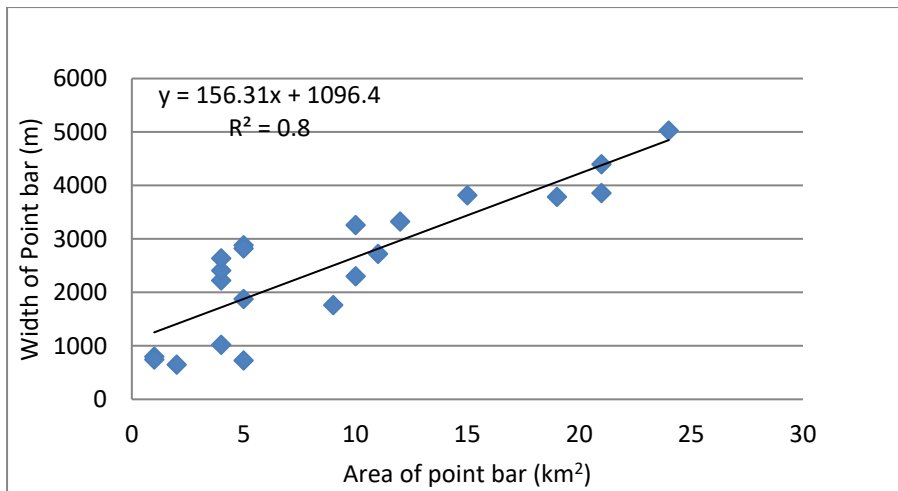
420

421 Figure 6: An example of point bars mapped along the River Niger (PB 04 to 07). These were then measured in
 422 ArcGIS to produce a quantitative characterisation of point bars in the Delta.



423

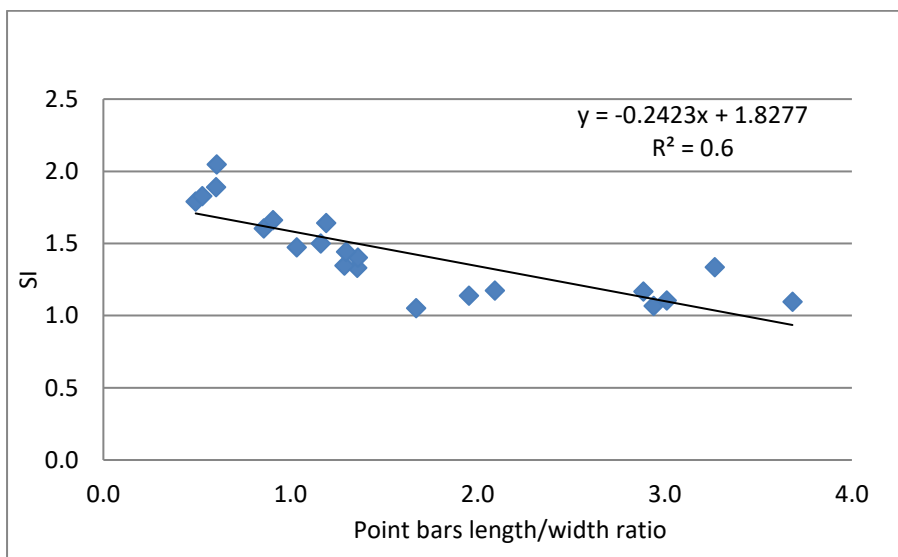
424 Figure 7: Plot length against the area of the point bar. The R^2 is 0.9; it shows a significant relationship between
 425 the length and the area of the point bars mapped, i.e. the larger the area the higher the length.



426

427 Figure 8: Plot of width against the area of the point bars. The R^2 is 0.8; it shows a significant relationship between
 428 the length and width against the area of the 24 point bars mapped, i.e. the larger the area the wider width.

429



430

431 Figure 9: Plot of Sinuosity Index (SI) against point bars length/width ratio. The R^2 is 0.6; it shows a significant
 432 relationship between the SI and the point bar length/width i.e. the SI and the point bar length/width ratio do depend
 433 on each other significantly for values of SI less than 2.0
 434

435

436 **4.5.5 Braid Bars, Bar Assemblages**

437 Braid bars are transient, they could change in shape and location based on a number of factors such as
 438 vegetation, the volume of water and sediments, slope gradient etc. (Bridge 2003, p. 149). Some could be
 439 submerged as the water level rises or exposed as it falls. Transient braid bars can split into small components of
 440 bar assemblage, while others might merge to form compound bar assemblages. The description of braid bar
 441 geometry is based on what was visible through the satellite images and will change with the natural evolving of
 442 the bars. However, it provides an overview of possible shapes and sizes that might be of relevance to subsurface
 443 studies. The mapped braid bars in the Niger Delta are grouped into four classes based on the landform they are
 444 associated with. These groups include: mid-channel bars, bank-attached bars, chute channel bars, and point bar-

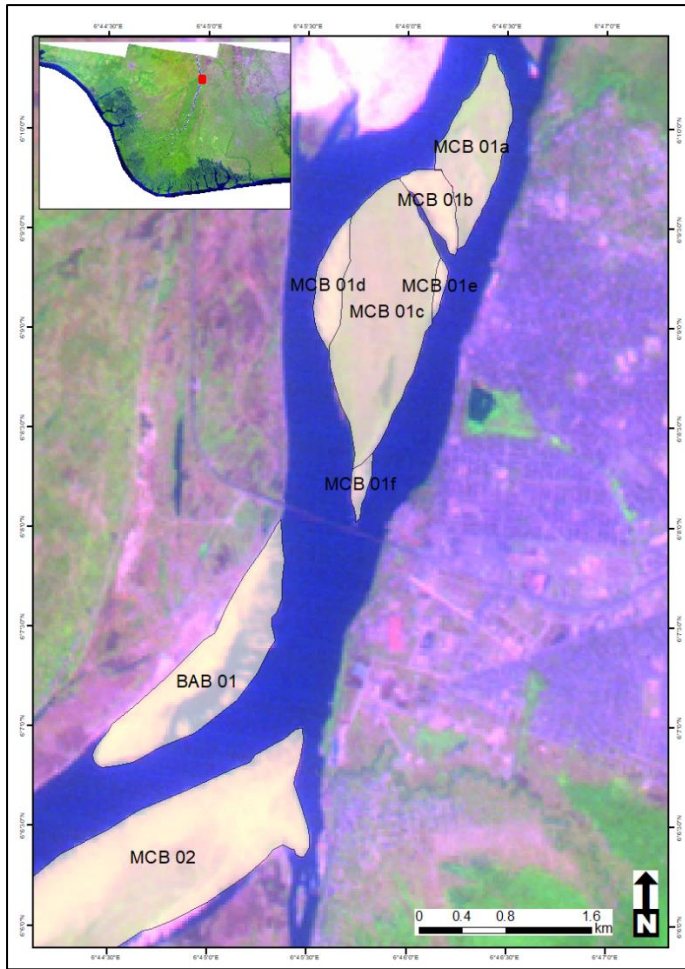
445 attached bars (Figure 10). The mid-channel bars are the most common feature, constituting 57% of the braid
446 bars in the Niger Delta. A total of 82 individual mid-channel bars were mapped out, of which 34 are associated
447 with fluvial channels and 48 with tidal channels. However, the bars associated with fluvial channels are the only
448 ones discussed here. The bank-attached channel bars are the second most common (27%), while the chute-
449 channel bars and the point bar-attached bars represent only 14% and 1% respectively of the entire population.
450 Figure 10 shows an example of a bar assemblage made up of mid-channel bar (MCB); MCB 07b-d. They seem
451 to have formed as a single bar, later separated by channels into MCB 01a, MCD 01d and MCB 01e. MCB 01e is
452 a new extension of the bars assemblage, while MCB 01a was a separate bar now merged with the other bars to
453 form a bar assemblage. BAB 01 is a new bar growth, though separated from the bank by chute channels. They
454 are classified as bank-attached bars as their build-up would have been initiated by the deposition at the bank.
455 MCB 02 appears to be separated from an island by anabranch channels on both sides.

456

457 The Niger River system is highly braided (simple braid bars) along its entire stretch. The Braiding Index (BI),
458 decreases downstream from 1.09 at its peak to 0.16 at the Forcados and Nun arms of the Niger River. There are
459 many parameters used by different authors to measure the Braiding Index (BI) (Egozi and Ashmore 2008),
460 including the Channel Count Index preferred by Egozi and Ashmore (2008). However, Friend and Sinha (1993)
461 method was used in this study because it also takes sinuosity into account. The L_{cmax} is the mid-channel length
462 of the widest channel through the reach and L_{ctot} is the sum of the mid-channel lengths of all the segments of
463 primary channels in a reach (entire channel length, which is more than 10 times the average channel width as
464 recommended by Egozi and Ashmore (2008)), and the Braiding Index BI is the braid channel ratio (L_{ctot}/L_{cmax}).

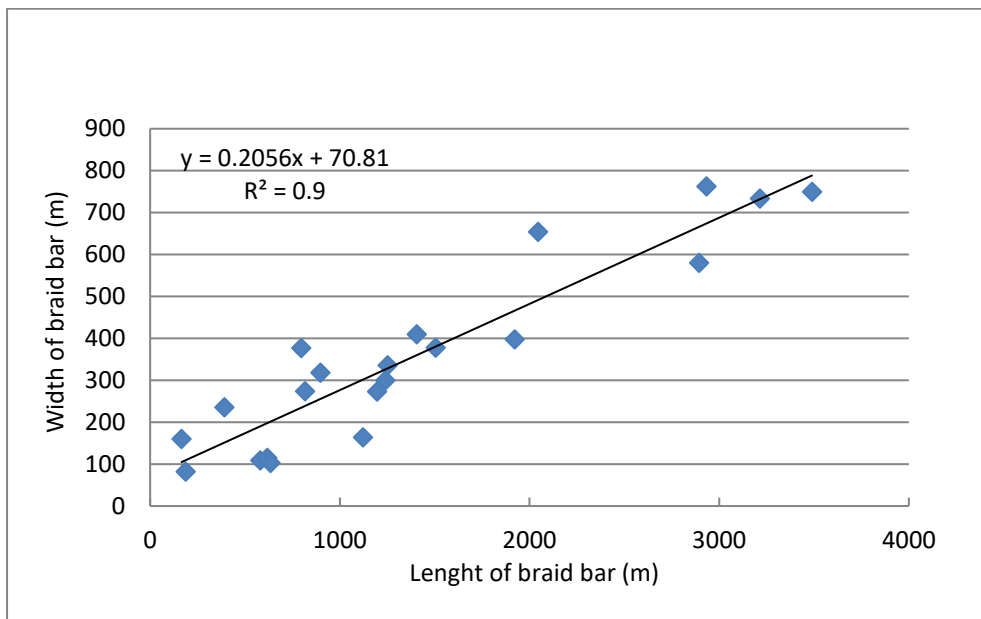
465

466 The area of mid-channel (fluvial) bars ranges from 0.012 km² to 6 km² (mode is 3 km²), the length ranges from
467 166 m to 8,053 m (mode is 1900 m) and the width from 82 m to 1,544 m (mode 120 m). The length to width
468 ratio ranges from 0.65 to 6.85. The area of mid-channel (tidal) bars ranges from 0.005 km² to 7 km², the length
469 ranges from 142 m to 5,972 m and the width from 54 m to 2,062 m. The length to width ratio ranges from 1.03
470 to 8.20. The coefficients of regression of the plot of braid bar length against width, length against the area, and
471 width against area fall between 0.8-0.9 mainly. The bar length and width are strongly correlated (Figures 11, 12
472 and 13). The observed outliers in some plots were associated with composite (amalgamated) mid-channel braid
473 bar. The results found here are comparable to those found elsewhere (Komar, 1984; Sambrook-Smith et al,
474 2005; Kelly, 2006), which again confirms that the relationship between bar length and width is scale-invariant.



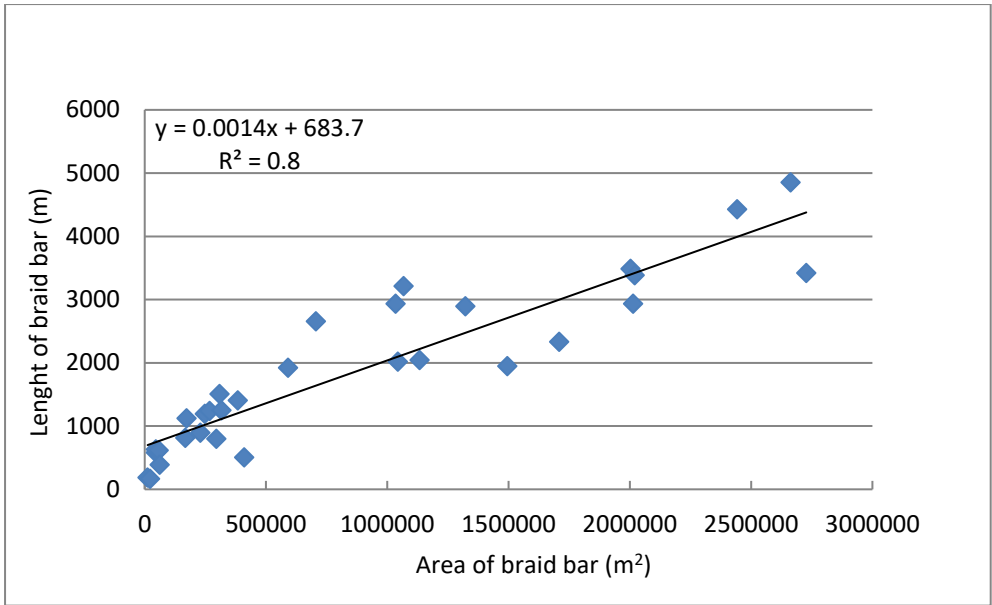
475

476 Figure 10: Section of River Niger showing two types of braided bars: bank-attached bars (BAB)
 477 bars (MCB).
 478



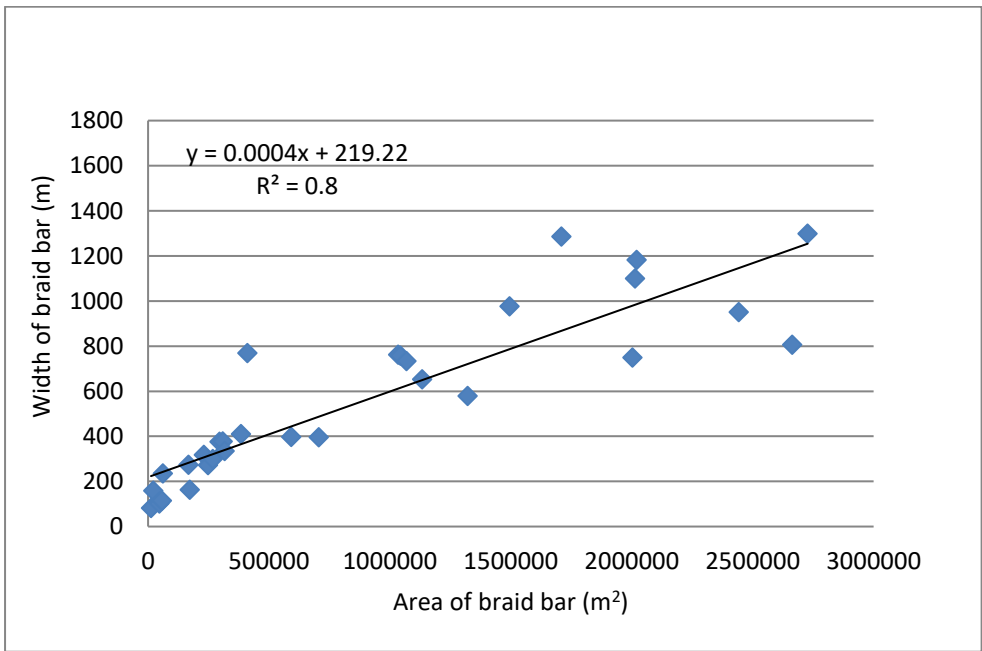
479

480 Figure 11: Plot of mid-channel bar width against length. The R^2 is 0.9; it shows a significant relationship between
 481 the width and length of fluvial mid-channel bars i.e. the width and length of fluvial mid-channel bars do depend
 482 on each other significantly when composite bars are excluded. Thus width-length relationship is stronger in single
 483 bars.



484
485
486
487
488
489

Figure 12: Plot of mid-channel bar length against the area. The R^2 is 0.8; it shows a significant relationship between the length and area of fluvial mid-channel bars i.e. the length and area of fluvial mid-channel bars do depend on each other significantly.



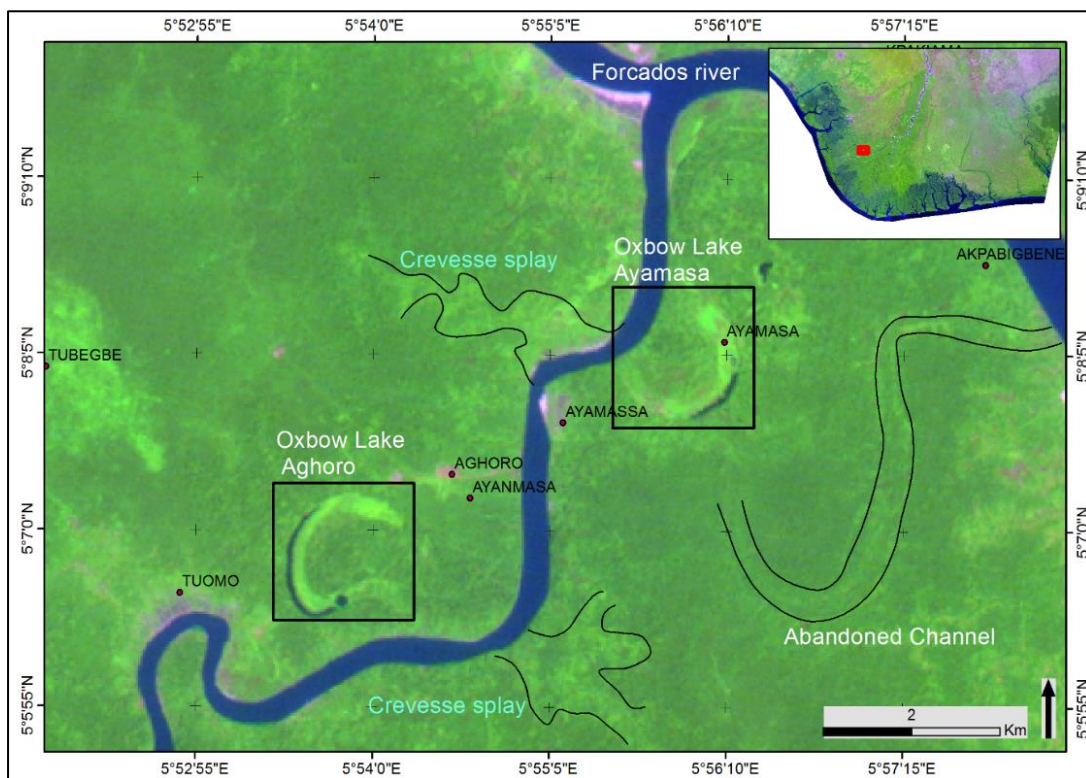
490
491
492
493
494
495

Figure 13: Plot of mid-channel bar width against the area. The R^2 is 0.8; it shows a significant relationship between the width and area of fluvial mid-channel bars i.e. the width and area of fluvial mid-channel bars do depend on each other significantly.

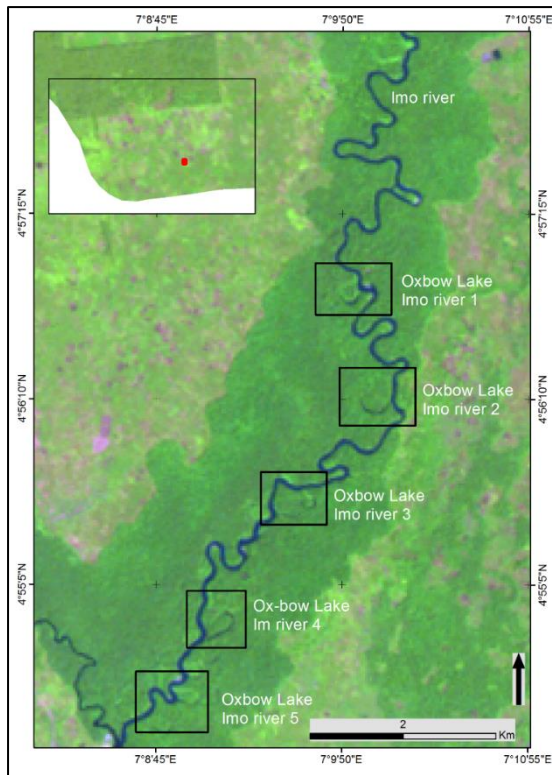
496 **4.5.6 Oxbow lakes.**

497 Oxbow lakes develop by a cut-off of a meander loop; they are usually filled with fine-grained floodplain deposits
498 or abandoned point bar deposits (Miall, 1992). Oxbow Radius of Curvature is the average distance from the
499 channel's bank at any point to the center of the ox-bow lake or point of intersection of two radii. It can be half the

500 oxbow diameter (Reading, 1996). Oxbow deposits exhibit a typical fining-upwards sequence (Erskine et al,
 501 1982). The oxbow lakes in the Niger Delta have a mean length of 2000 m and its width ranges from 32 m to 500
 502 m with an average width of 135 m and mode of 162 m. The radius of curvature ranges from 32 m to 1432 m as
 503 shown in Figure 14 and 15. Oxbow lakes in the Niger Delta are mostly located at Aghoro and Ayamasa, while
 504 other small-scale ones are observed in the upper floodplain. Most oxbow lakes tend to be found outwards from
 505 the axial region, where the channels are very sinuous. For example, oxbow lakes were observed along the channel
 506 of the Imo River, which has a very high sinuosity (SI of 3.0 and above). The geometry of oxbow lakes in the Niger
 507 Delta conforms to that in the Mississippi Delta described by Holbrook and Alexandrowitz (2011).
 508
 509 Constantine and Dunne (2008) observed that oxbow lakes are produced by meander cut-off, which correlates
 510 with sinuosity. Dieras et al (2013) explained that topography can influence flooding and cutoff channel initiation
 511 as well. In particular, it has been observed that where the topography is low, overflowing is more frequent and
 512 cutoff and oxbow lakes are more likely to occur (also see Fagan and Nanson, 2004). That is why most Niger
 513 River oxbow lakes are also associated with channels in low relief areas of the lower delta plain. Oxbow lakes
 514 are generally filled with fine sediment, within which lenses of coarse sediment are contained. Once buried, these
 515 have significant reservoir implications as the fine sediments can act as clay plugs (Dieras et al, 2013).



516
 517 Figure 14: A satellite image showing Oxbow lakes at Ayamasa and Aghoro, from a section of Forcados River.
 518



519

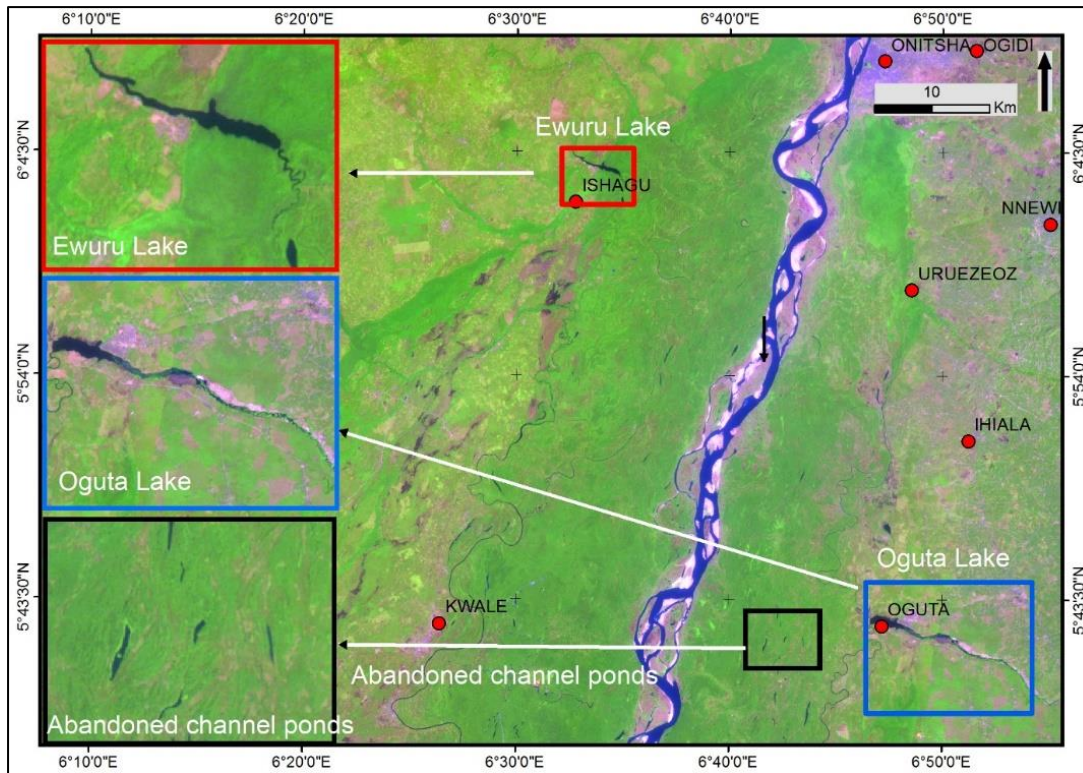
520 Figure 15: A satellite image showing the Imo River where the sinuosity of the channels that are long and narrow
 521 is generally higher than 2.0. There is also a progressive increase in sinuosity with stream order, particularly from
 522 first to third order.
 523

524 **4.5.7 Other lakes, Ponds and Cut-Off Channels**

525 Other lakes and ponds are frequent in the Niger Delta, and include, amongst others, Ewuru Lake in the west and
 526 Oguta Lake in the east, the largest lakes in the Niger Delta (Figure 16). A pond is a naturally-standing body of
 527 water that is usually smaller than a lake. They may occur in floodplains or abandoned channels (Keddy, 2010)
 528 either isolate or part of a river system. Ewuru Lake is 8 km long and 300 m wide; Oguta Lake is 20 km long,
 529 with an average width of 600 m. The two lakes are elongated along a similar orientation, about 115°N in
 530 azimuth, which differs from the general N-S orientation of most Niger Delta channels (fluvial and tidal). It is
 531 possible that the lake orientation is controlled by the structural influence of underlying regional faults that
 532 separate the depobelts in the Niger Delta (Doust and Omatsola, 1990, Stokes and Mather., 2003, Roberts et al,
 533 2012). These trend east-west and run parallel to the coastline. Most other lakes and ponds are found within the
 534 upper floodplain and are shorter, with lengths ranging from 800 m to 3000 m, while their width ranges from 90
 535 m to 280 m. They are interpreted as abandoned cut-off channels of the Niger, Ase, and Orashi rivers as they are
 536 aligned in the same direction of flow of these rivers (N-S). They could also play a role in draining the floodplain
 537 during and after flooding (Fagan and Nanson, 2004).

538

539



540
 541 Figure 16: Satellite image of the Ewuru and Oguta lakes, other lakes, ponds, and cut-off channels.

542
 543

544 **4.6 Geometries of landforms associated with the lower deltaic plain and delta front**

545 Distinct landforms, such as tidal channels (estuarine), beaches and spits braid bars, were mapped in the lower
 546 delta plain and measured. The dimension and spatial distribution of these landforms, especially those at the
 547 coastal margin, was also used to inform their classification, using Ainsworth et. al (2011) plan-view
 548 morphodynamic model. This is a classification model in which the relative influences of tidal, wave and fluvial
 549 processes are inferred, looking at the architecture of the landforms and/or either the absence or presence of some
 550 components of the landform assemblage (Ainsworth et. al., 2011, and Vakarelov and Ainsworth, 2013). For
 551 example, a tidal channel having tidal flats present or absent could indicate the influence of tidal or fluvial process
 552 respectively, whereas the presence of beaches indicates the influence of wave processes.

553

554 **4.6.1 Tidal channels (Estuarine)**

555 The most common morphological elements of the swamp area are the main tidal channels, creeks and inter-creek
 556 flats (Figures 17, 18a-d). The tidal channels are typically straight or gently curved and are aligned perpendicular
 557 to the coast with the depth ranging from 9 to 15 m (Oomkens, 1974). Many are direct extensions of upland rivers,
 558 carrying a mix of fresh and salt water. Smaller meandering creeks interconnect these major tidal channels. The
 559 network of tidal channels and creeks breaks up the swamp into a jig-saw of irregular-shaped tidal flats bordered
 560 by deep channels, which flood and drain the tidal flats. The inter-creek flats have low relief and show dendritic
 561 patterns. These may stem from the densely-vegetated tidal flats (Allen, 1965). At slack tides, the creek waters
 562 become still, so that clay-silt floccules, suspended in the brackish waters, become deposited. Once deposited, these
 563 cohesive fines are difficult to remobilise and erode.

564 To establish the fluvial, tidal and wave influence on these landforms, we looked at the presence or absence of
565 beaches at the delta front, mouth bar and tidal flat within the tidal channel and whether tidal channel terminated
566 at the bay-line or are connected to the fluvial channel in the upper deltaic plain. Comparing these to the template
567 by Boyd et al. (1992) model, Ainsworth et. al. (2011), and Vakarelov and Ainsworth (2013), the results show
568 that the overall geomorphic expression of the processes of river, tide and wave varies per group of tidal channels
569 across the delta, dividing it into zones that fit into different parts of the ternary system or category of delta
570 classification:

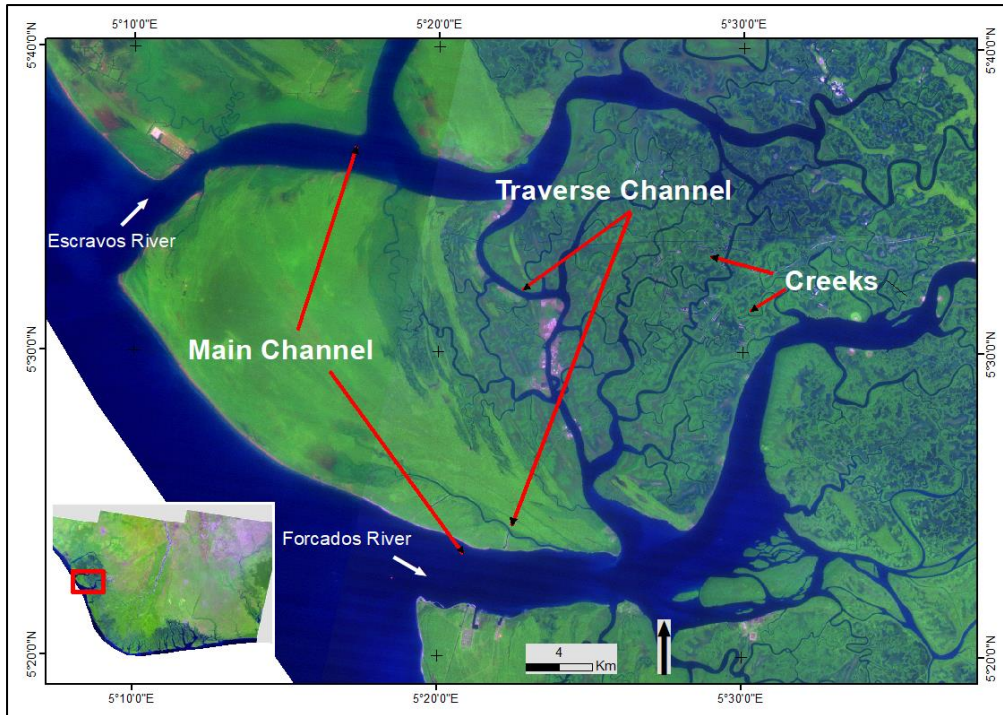
571

- 572 1. Tide-Wave channels are most common to the west, an area characterised by wide beach ridges,
573 disconnected tidal channels, evidence of sediment starvation, and the absence of mouth bar. Boyd et al.
574 (1992) model captured this region as progradational and affected by wave and tidal power. The area is not
575 tide-dominated but tide-influenced (after Hori and Saito 2007). It is classified as **Tw**, i.e. tide-dominated
576 and wave-influenced, following Ainsworth et al. (2011) (Figures 18a and b).
- 577 2. Fluvial-Wave channel landforms are present towards the centre of the lower delta plain, an area
578 characterised by narrow, almost absent beach ridges, connected tidal channels, and spits. In Boyd et al.
579 (1992) model, this region is considered progradational, affected by decreasing wave and tidal power but
580 increasing fluvial power and sediment supply. Using Ainsworth et al., (2011) classification, this area
581 would be classified as **Fw** (i.e. fluvial-dominated and wave-influenced, Figure 18c).
- 582 3. Tide-Wave channel landforms are typical of the east, where wide beach ridges, wide disconnected tidal
583 channels and signs of sediment starvation are common, while there is no mouth bar. In Boyd et al. (1992)
584 model, this area can be considered progradational, with an increasing wave and tidal power). Using
585 Ainsworth et al., (2011) classification, it is **Tw** i.e. tide-dominated and wave-influenced (Figures 18a and
586 b).
- 587 4. Tides are the dominant process to the Far East channel, where no beaches are found but transgressive tidal
588 flats are present. Cross and Rio del Rey rivers are high-energy transgressive estuaries (Whiteman 1982). In
589 Boyd et al. model (1992) model this region fits into the tide-dominated estuary class, which is
590 transgressive with increased tidal power. In Ainsworth et al., (2011) classification the area will be classed
591 as **Tf**, i.e. tide-dominated and fluvial-influenced (Figures 18d).

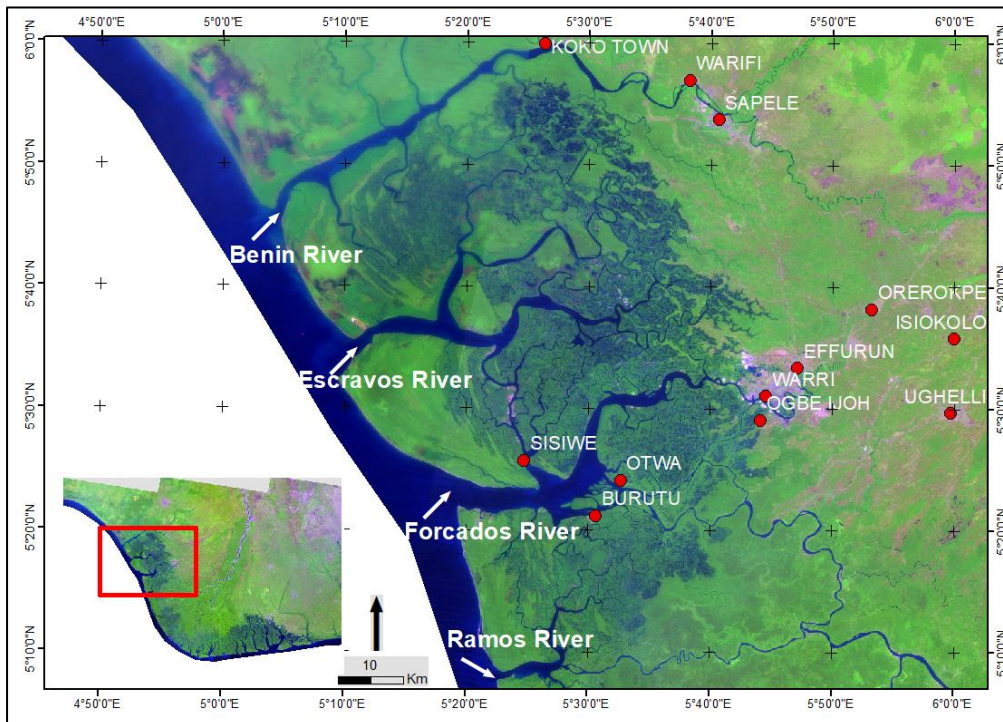
592

593 Although, we have divided the Niger Delta into four zones with each zone having a unique landform in response
594 to the dominant delta forming process(es), the overall geomorphic expression of these processes of river, tide
595 and wave across the entire Niger Delta is considered as a sum of the processes in the four subzones. Therefore,
596 in the context of Ainsworth et. al. (2011), and Vakarelov and Ainsworth (2013) model, using the landforms of
597 the lower-delta plain and delta front, the Niger Dela is essentially classified as tide-dominated, wave-influenced
598 and fluvial-effect (**Twf**). This implies that the Niger Delta is classified as a mixed delta using the tripartite model
599 in agreement with previous publications (Short and Stable 1967, Doust and Omatsola, 1990)

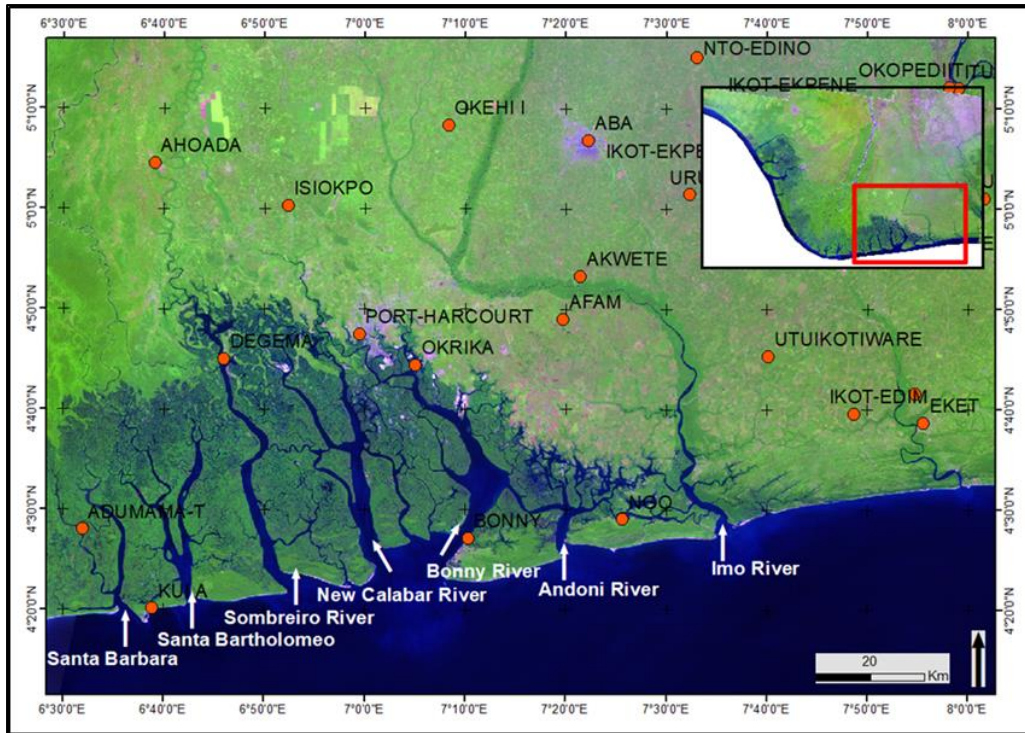
600



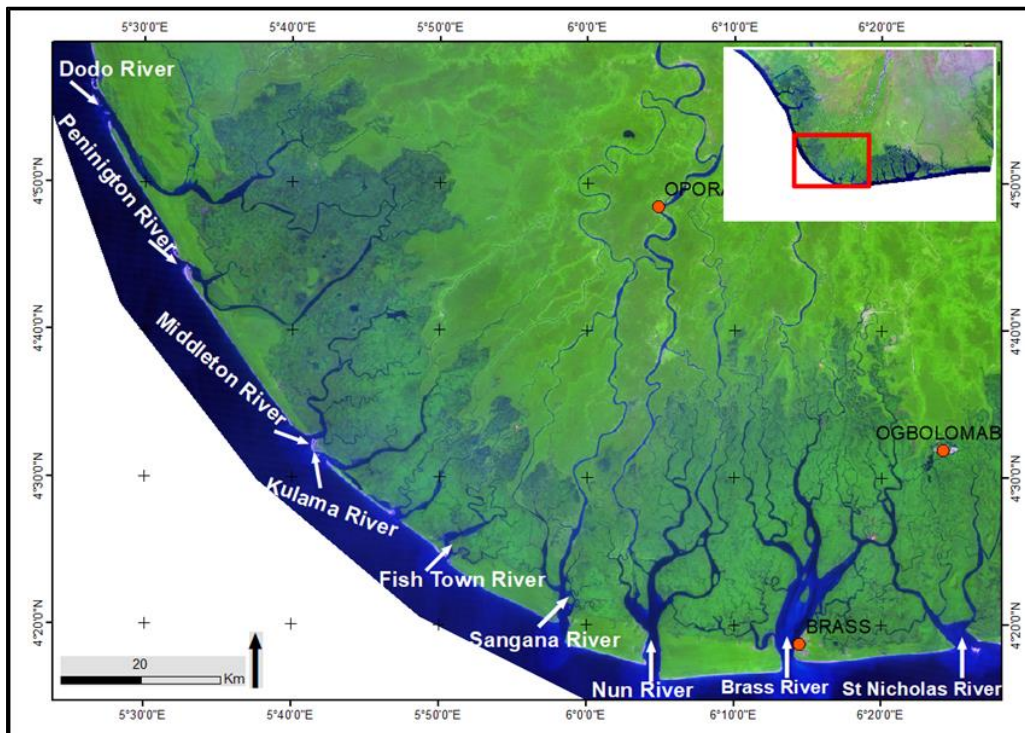
601 Figure 17:
 602 Western tidal channels: part of the lower delta plain and delta front showing the channel style of the main tidal
 603 channel running perpendicular to the coastline.
 604



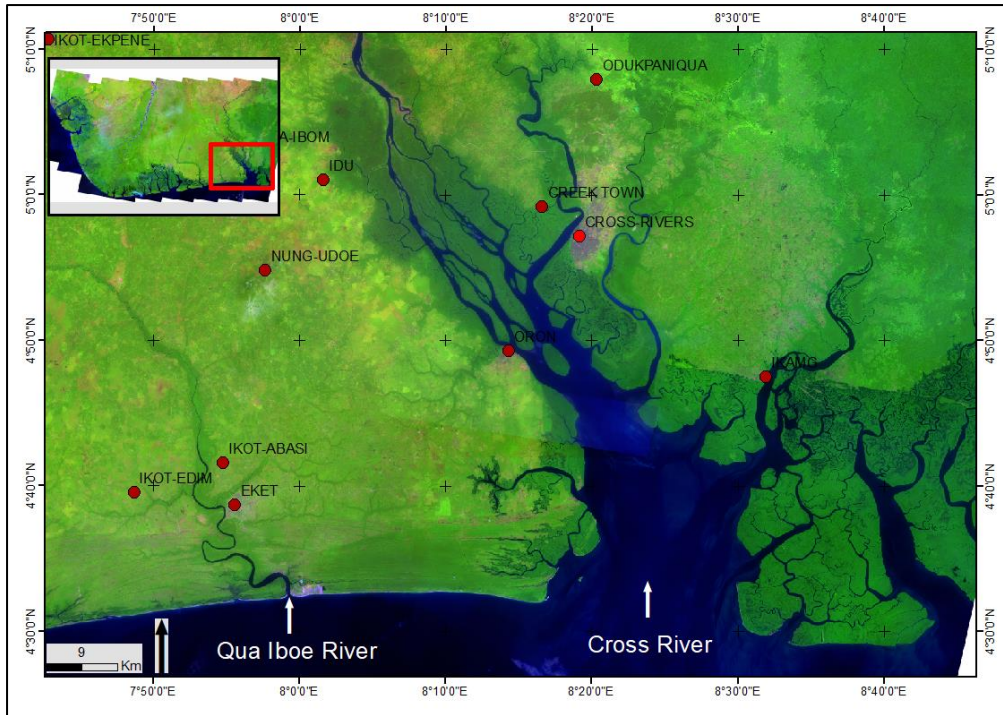
605
 606 Figure 18a: A satellite image of the western tidal channels (in blue). These are wider than the central tidal
 607 channels in Figure 18c. This is due to the impact that high tides have on these western channels because they are
 608 connected to abandoned channels and therefore starved of sediment supply, it is classified as **Tw**, (i.e. tide-
 609 dominated and wave-influenced, following Ainsworth et al. 2011).
 610



611
 612 Figure 18b: A satellite image showing the eastern tidal channels (in blue). These are wider than the central tidal
 613 channels in Figure 18c because are connected to abandoned channels, and therefore are starved of sediment
 614 supply and more strongly impacted by the action of high tides. it is classified as **Tw**, i.e. (tide-dominated and
 615 wave-influenced, following Ainsworth et al. 2011).
 616



617
 618 Figure 18c: A satellite image showing the central tidal channels. These are narrower than the western and
 619 eastern tidal channels in Figures 18a and b. The tidal channels at the central part of the Niger Delta are directly
 620 connected to fluvial channels (active) that supply sediment into the ocean through them. With high sediment
 621 supply, the impact of the tide in widening them is reduced, thus channels in this zone of high sediment
 622 flux are narrower. It is classified as **Fw** (i.e. fluvial-dominated and wave-influenced, following Ainsworth et al. 2011).



623 Figure 18d: Far-East channels showing the channel style of the main tidal channel running perpendicular to the
 624 coastline. The widest shows evidence of tidal flats which indicates high tidal impact with no obvious evidence
 625 of wave impact. it is classified as **Tf**, (i.e. tide-dominated and fluvial-influenced, following Ainsworth et al.
 626 2011).
 627

628
 629 **4.6.1.1 Tidal channels width variation**

630 Tidal channel width variation along the channel profile was plotted for 21 tidal inlets. The results from these
 631 plots (Figure 19) shows that width of the tidal channels reduces exponentially upstream (see the relationship in
 632 equations), moving from the coast, where the width is widest, towards the channel head. In contrast, fluvial
 633 channel width decreases downstream linearly. This is a key characteristic to distinguish tidal and fluvial
 634 channels in the Niger Delta and can be of relevance in understanding the paleogeographic context of subsurface
 635 deposits. Similar trends have been identified elsewhere (Wright et al., 1973; Pethick, 1984; Eisma, 1998;
 636 Fagherazzi & Furbish, 2001; Harris et al., 2002; Marani et al., 2002; Davies & Woodroffe, 2010; Hughes,
 637 2012). The relationship between tidal channel width and distance along the channel for the Niger Delta can be
 638 summarised as:

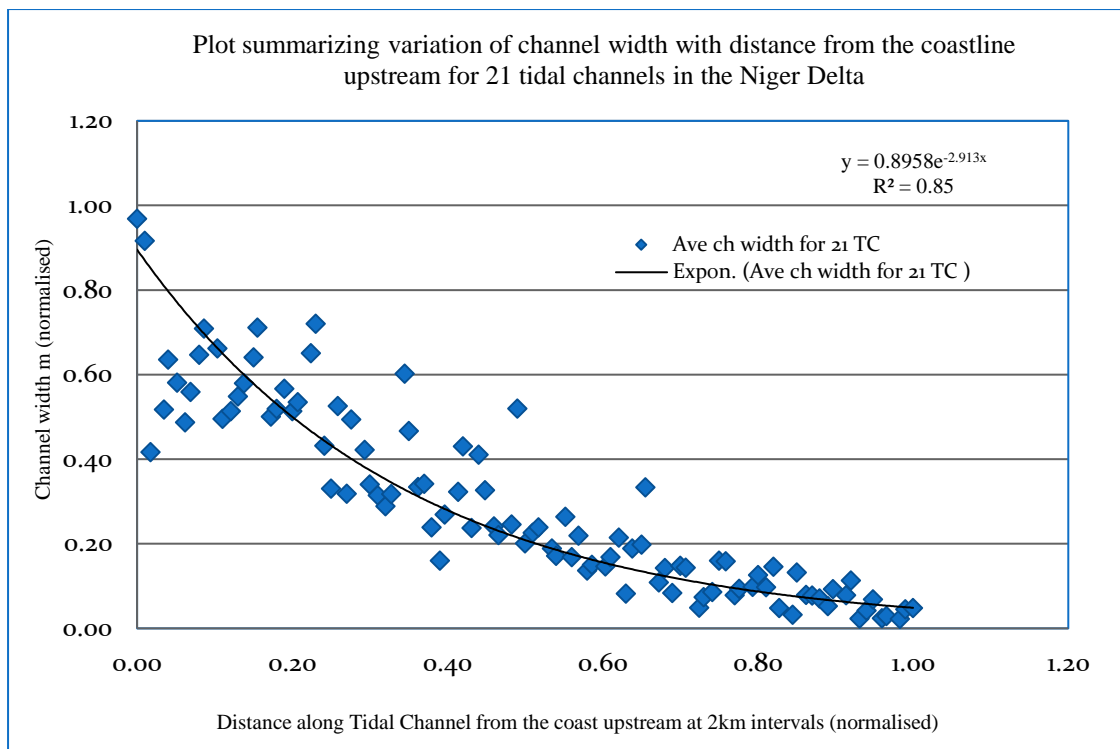
639
 640
$$Y=0.8952e^{-2.913x}$$
 Equation 2

641
 642 Equation 3 is the general form of Equation 2

643
$$Y=W_m e^{-rx}$$
 Equation 3

644
 645 Where

- 646 Y = Tidal channel width at any point along the channel
- 647 W_m = Tidal channel mouth width (547 m-6000 m, mostly 1000 m-5000 m)
- 648 x = Distance along channel
- 649 r = Rate of change of channel width



650

651 Figure 19: Plot summarizing variation of channel width with distance from the coastline upstream for 21
 652 tidal channels in the Niger Delta

653

654 **4.6.2 Beaches, Barrier bars and Islands**

655 The ridges and swales have been constructed by the lateral or offlap accretion of successive sediment layers
 656 culminating in low ridges (Figure 20). In general, the youngest set of ridges and swales closest to the sea are
 657 sparsely covered by vegetation, having been impacted upon by strong wave action. The outer meander bank is
 658 generally high and steep, commonly showing a section in levee or backswamp sediments. The beach ridges are
 659 separated, one from another, by deep tidal ebb-flood channels leading to the swamps. The entire coastal margin
 660 of the Niger Delta is rimmed with elongate beaches and barrier islands (as reported by Allen 1965, Whiteman,
 661 1982). There are 20 beach ridges separated from each other by tidal inlets, as shown in Figure 20.

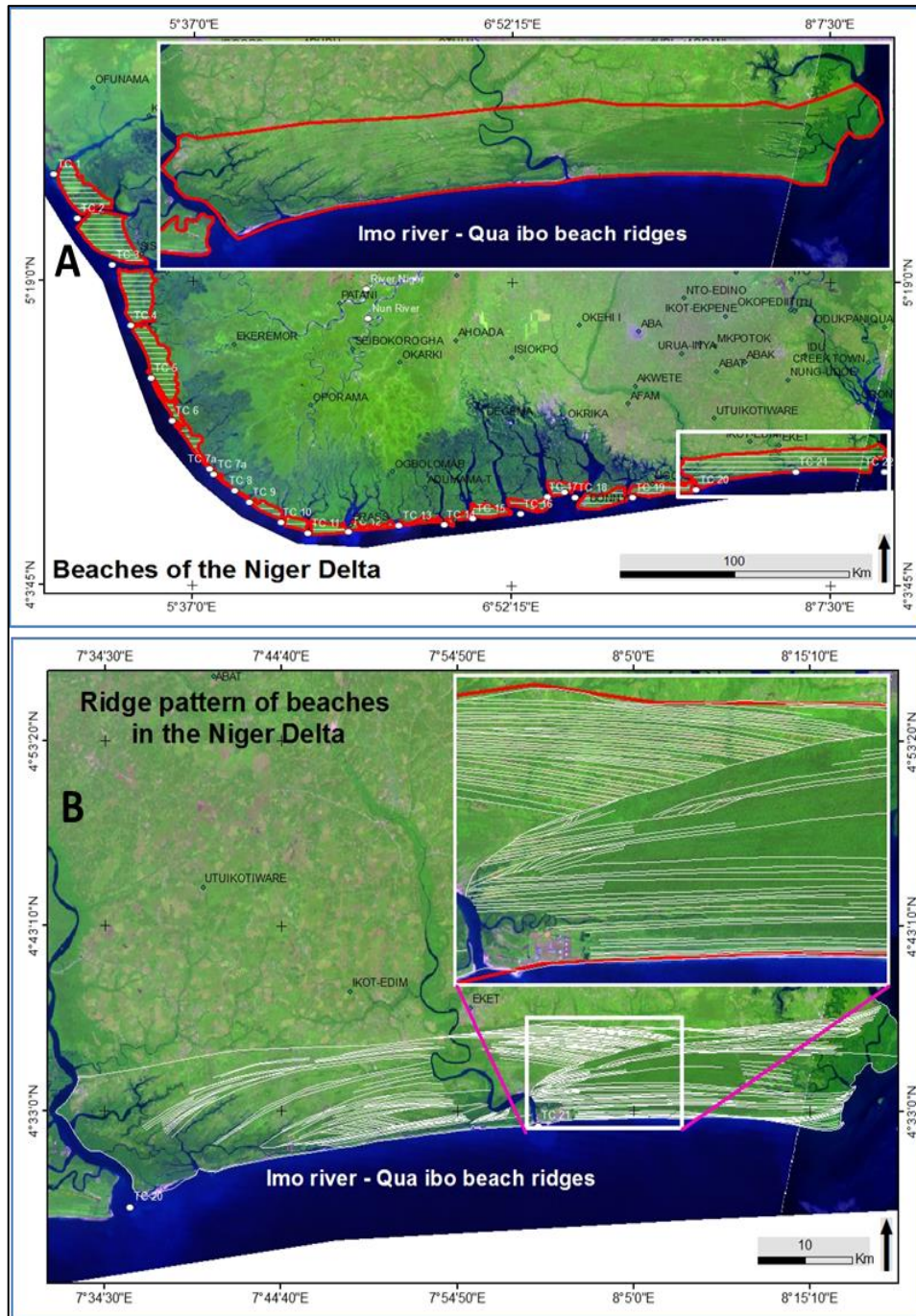
662

663 These beaches are longer and wider on the eastern and western flanks and thin-out in length and width towards
 664 the centre of the delta coastline. The beaches are narrower in the central part because fluvial action is predominant,
 665 while at the flank tide and wave processes are predominant and support beach formation. Beaches are completely
 666 absent in the far-east Cross River; the tidal action is predominant here as compared to any other part of the Niger
 667 Delta coastline. The beach ridges are important because they indicate progradation of strand plain (ancient
 668 coastlines) and thus are associated with sea level fluctuation (Otvos, 2000).

669

670 The ridge and scroll orientation in all the beaches are parallel to the coastlines, except the Imo-Qua-Ibo beach
 671 (Figure 20-part B) that displays more than three distinct sets of accretion ridges. This is interpreted to have been
 672 formed at different times and a possibly different set of environmental conditions. The Cross-River supplies most
 673 of the sediment to this region. The area is characterised by tides higher than 4 m (macrotidal), whereas other

674 regions have tides lower than 2 m (microtidal to mesotidal) (Oomkens, 1974); this could account for the difference
 675 in overall morphology of the tidal inlets too. Tidal channels' width ranges from a few hundred meters to 12 km
 676 but is mostly about 5 km. The larger ridges, consisting of bundles of the smaller ones, are as long and reach widths
 677 of 1.5 km.
 678



679
 680 Figure 20: **A-** Mapped beaches in the Niger Delta. Insert: Imo-Qua-Ibo Beach. **B-**Imo-Qua-Ibo Beach; the
 681 longest and the most complex with more than three generations of accretions ridges (i.e. ridges are different in
 682 pattern and directions unlike the rest in the Niger Delta)

683
 684 **4.6.3 Spit**

685 Spit landforms were observed and mapped in the central part of the Niger Delta coastline (Figure 21). Spits are
686 the physical expression of wave actions and longshore drifts. They grow in the direction of littoral drift forming
687 larger beach ridges with time., It is suggested that the smaller ridges result either from changes in sand supply
688 along the beaches or from the march of offshore bars onto the exposed beach (NEDECO, 1954; 1961). Spits record
689 major changes in the shape of the coast resulting from changes in river and the tidal regime, the direction of wave
690 attack, and sand supply. The breaking swell releases much physical energy on the beaches. Sand is incorporated
691 into the beaches wherever made available to the wave-generated longshore currents.

692

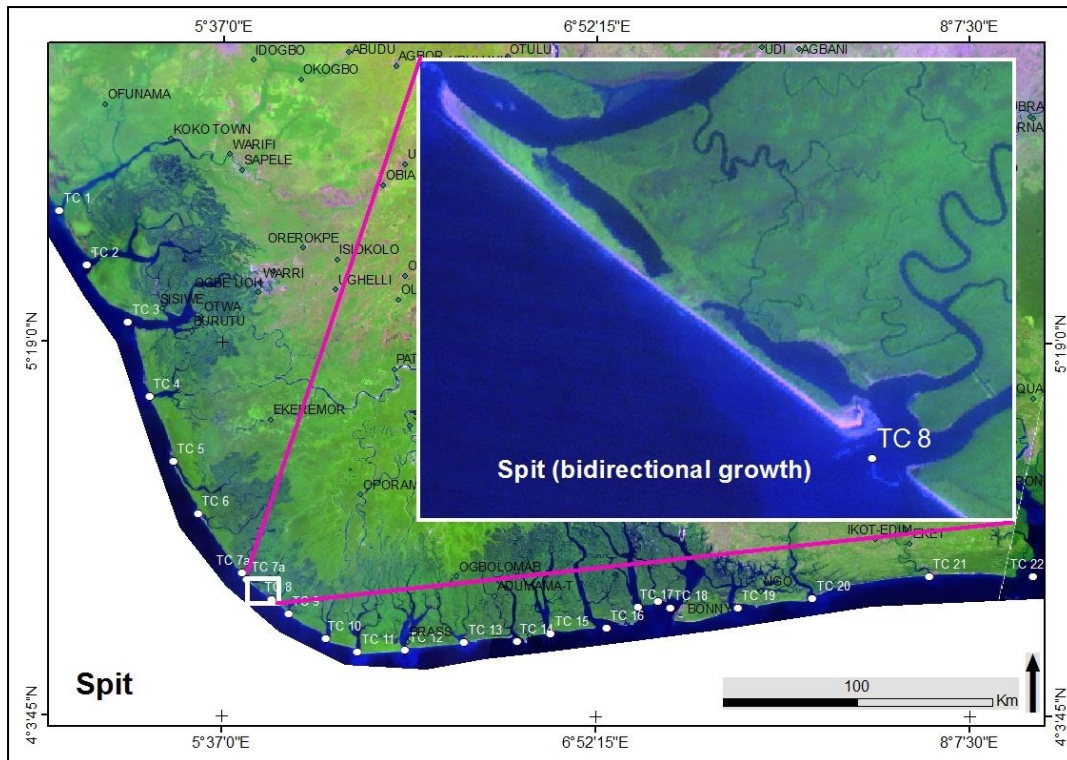
693 The presence of spits in the Niger Delta indicates that the delta morphology is influenced by waves (Ashton and
694 Giosan 2007, Bhattacharya and Giosan, 2003). They are of concern in this study because of the role they play in
695 sediment redistribution and on delta morphology. Spit bidirectional morphology (Figure 21) shows that the
696 longshore drift in the Niger Delta is bidirectional (this paper, Allen 1965; Whiteman, 1982).

697

698 As the wave action hits the coastline at the apex, it diverges to the east and west causing sediment redistribution
699 with a strength of wave force and longshore current strong enough to override tidal influence in this region. As
700 the spits grow, they tend to cover the channels and subsequently increase the angles of the channels to the
701 coastline. This, in turn, reduces the dispersive impact of tides on one hand and increases delta progradation from
702 sediment influx from the river on the other hand (Ashton and Giosan 2007, Wright and Coleman, 1973;
703 Bhattacharya and Giosan, 2003). The horizontal distance between tide marks ranges typically from 50 to 150 m,
704 and the slope of the intertidal part of the beach generally ranges from 1:100 to 1:50 (NEDECO, 1954, p. 84).

705

706 Using the FitzGerald et al. (2001) model the spit accretion in the Niger Delta fits into the “Time 1; Inlet
707 Migration and Spit Breaching”, while most of the other tidal inlets fit into the “Time 1; Stable Inlet Processes”.
708 In both cases, sand bypasses the tidal inlet (FitzGerald et al., 2001; FitzGerald et al., 2012). Also, using the tidal
709 asymmetry model by Bhattacharya & Giosan (2003) for the classification of wave-influenced deltas, tidal inlet
710 morphology in the Niger Delta shows that fluvial, tidal and wave influence varies along the coastline. Most tidal
711 inlets at the central part of the Niger Delta fit into the asymmetric and deflected end members (Figure 18c),
712 which indicates higher sediment discharge and longshore drifts and is typical of deltas preserving a lower
713 proportion of fluvial-derived mud (Bhattacharya & Giosan, 2003, Bhattacharya, 2006; 2010). At the flanks, the
714 inlets fit into the second row-symmetric (Figures 18a and 18c), an indication of deltas comprising more
715 heterolithic deposits. This is a clear indication of the differential influence of the river sediment discharge and
716 the dispersive effect of the longshore drift. The morphology and spatial distribution of the landforms (tidal
717 channels, beaches and spit) were used to characterise each coastal zone, following the delta ternary classification
718 and the asymmetry and spit accretion models of Bhattacharya & Giosan (2003) and FitzGerald et al., (2001).



719
 720 Figure 21: Bidirectional spit development at the apex of the Niger Delta. Spit development is common in the
 721 central part of the Niger Delta.
 722

723
 724 **5 Summary and Conclusion**

725 The sedimentary environments in the Niger Delta include a mix of fluvial, tidal and wave-related deposits and
 726 landforms, thus indicating that the Niger Delta is a mixed delta. The extent of the delta has been revised from
 727 the original works of Allen (1965) and Short and Stauble (1967). Analysis from this study reveals that the area
 728 of the entire Niger Delta is 70,000 km², of which the upper deltaic, lower deltaic and delta front portions are
 729 69%, 25%, and 6% respectively.

730
 731 Each of these three main environments is characterised by distinct sedimentary and geomorphological processes
 732 and landforms. Therefore, using Ainsworth et. al. (2011) and Vakarelov and Ainsworth (2013) model and
 733 applying it to the landforms of the lower-delta plain and delta front, the Niger Delta is essentially classified as
 734 tide-dominated, wave-influenced and fluvial-effect (Twf).

735
 736 The upper delta plain is further divided into: dry flat land, upper floodplain, lower floodplain, and the abandoned
 737 channel zone. The dimensions and spatial analysis of each of these zones revealed that they are mostly
 738 influenced by fluvial activities, unlike the lower delta plain and delta front that are dominated by tidal and wave-
 739 related activity respectively.

740
 741 Also, the geometric analysis of constituent landforms in these zones indicates that the fluvial channel width
 742 reduces downstream linearly, contrary to the tidal channel width that increases exponentially downstream. Point
 743 bar width and length, as well as point bar width and channel width, show strong correlation and dependence.

744 Also, braid bars width, length, and area show strong correlation and dependence with each other. The width of
745 the upper floodplain is fairly constant, implying that the change in its ratio (floodplain width to channel width,
746 along the same path) downstream is not controlled by the change in channel width. Therefore, the variation of
747 floodplain width does not depend on the width of the channel that floods them.

748

749 The orientation of most cut-off channels follows the dominant N-S orientation of the whole delta system.
750 However, the two largest lakes of the area, Ewuru, and Oguta lakes, follow an E-W orientation, likely controlled
751 by the underlying E-W regional faults of the Niger Delta.

752

753 Overall, results from this study offer invaluable information on the spatial distribution and dimensions of these
754 sedimentary environments. The ratios and correlations of the dimensions of these sand bodies remain scale-
755 invariant, regardless of the variations in their size. The geometry and spatial distribution of these geobodies are
756 not only ideal to develop and/or test geomorphological models attempting to predict the evolution of deltas
757 (dominance, influence or effects of delta forming processes) but they are also vital in predicting the distribution
758 of sand bodies in the subsurface. The dimensional analysis of individual sand bodies is key in reservoir
759 modelling to constrain facies proportions and to estimate the unknown dimension based on the statistical
760 relations presented here. This study is particularly important because the results can be used as analogue with
761 which the geometry and distribution of buried landforms can be constrained, within and beyond the Niger Delta.

762

763 **6 Acknowledgment**

764 Chinotu Franklin George would like to thank his sponsor: Petroleum Technology Development Fund (PTDF)
765 and SPDC Port Harcourt for providing the satellite images used. He expresses his gratitude to his mentors: Dr.
766 K. O. Ladipo and late Professor L. C. Amajor, and to Ms. Okwuchi Omekara for the technical support, she
767 offered for data assembly.

768

769

770 **7 References**

- 771 Allen, J. R. L., 1963. Sedimentation in the modern delta of the Niger River, West Africa, in Van Straaten L.M. J.
772 U. (ed.), *Deltaic and shallow marine sediments*: Amsterdam, Elsevier Publishing Co., p. 26-34.
- 773 Allen, J. R. L., 1965. Late Quaternary Niger Delta and adjacent areas; sedimentary environments and lithofacies,
774 *American Association of Petroleum Geologist, Bulletin*, vol. 49, p. 547-600.
- 775 Allen, J. R. L., 1970. Sediments of the modern Niger Delta: A summary and Review, In Morgan (ed) *Deltaic*
776 *sedimentation*, Society for Economic Palaeontologists, *SEPM Special Publication*, p. 138-151.
- 777 Allen, J. R. L. and Wells J. W., 1962. Holocene coral banks and subsidence in the Niger Delta, *Journal of*
778 *Geology*, vol. 70, p. 407-422.
- 779 Ashton, A. and Giosan, L, 2007. Investigating plan-view asymmetry in wave-influenced deltas, *River, Coastal*
780 *and Estuarine Morphodynamics 5th IAHR Symposium, Enschede, The Netherlands*.
- 781 Asseez, L. O., 1989. Review of the Stratigraphy, Sedimentology and Structure of the Niger Delta, In: Kogbe C.
782 A. (ed), *Geology of Nigeria*, Lagos, Elizabethan Publishing Co. p. 311-324.

783 Avbovbo, A. A., 1978. Tertiary Lithostratigraphy of Niger Delta, *American Association of Petroleum Geologist,*
784 *Bulletin*, vol., 62, p. 295-306.

785 Berendsen, H.J.A., Cohen, K.M. and Stouthamer, E., 2007. The use of GIS in reconstructing the Holocene
786 paleogeography of the Rhine-Meuse delta, The Netherlands. *International Journal of Geographical*
787 *Information Science*, 21, 589-602. <http://dx.doi.org/10.1080/13658810601064918>

788 Ainsworth, R. B., Vakarelov B. K., and Nanson R. A., 2011, Dynamic spatial and temporal prediction of changes
789 in depositional processes on clastic shorelines: Toward improved subsurface uncertainty reduction and
790 management, *AAPG Bull*, 95 (2), 267-297, DOI:10.1306/06301010036.

791 Bhattacharya, J.P., and Giosan, L., 2003. Wave-influenced deltas: geomorphological implications for facies
792 reconstruction: *Sedimentology*, v. 50, p. 187–210.

793 Bhattacharya, J.P., 2006, Deltas, In: Walker, R.G., and Posamentier, H., (eds.) *Facies Models revisited*, SEPM
794 Special Publication, v. 84, p. 237-292.

795 Bhattacharya J.P., 2010, Deltas, in: *Facies Models 4*. Dalrymple R.G. and James N.P., (eds). Geological
796 Association of Canada. *Geotext*, v. 6, p. 233-264.

797 Blum, M. D., and Roberts, H. H., 2009. Drowning of the Mississippi Delta due to insufficient sediment supply
798 and global sea-level rise. *Nature Geoscience*, 2(7), 488-491.

799 Borer, J. M., and Harris P. M., 1991. Depositional facies and cyclicity in the Yates Formation, Permian Basin-
800 Implications for reservoir heterogeneity: *AAPG Bulletin*, v. 75, p. 726-779.

801 Bridge, J.S., 2003. *Rivers and Floodplains: Forms, Processes, and Sedimentary Records*, United Kingdom,
802 Blackwell Publishing. p. 1-13, 141-328.

803 Bryant, I.D. and Flint, S.S., 1993. Quantitative clastic reservoir geological modelling: Problems and perspectives.
804 In: *The Geological Modelling of Hydrocarbon Reservoirs and Outcrop Analogues*, pp. 3–20 (eds Flint, S.
805 and Bryant, I.D.). International Association of Sedimentologists Special Publication 15, Blackwell
806 Scientific Publications, Oxford.

807 Burke, K. C., and Whiteman, A. J., 1973. Uplift, rifting and the break-up of Africa. In: Tarling, D.H., Runcorn,
808 S.K. (Eds.), *Implications on Continental Drift to Earth Sciences*, pp. 735–755.

809 Burke, K.C. and Dewey, J.F., 1974. Two plates in Africa during the Cretaceous? *Nature London* 249, 313–316.

810 Constantine, J.A. and Dunne, T., 2008. "Meander cutoff and the controls on the production of oxbow lakes",
811 *Geology*, vol. 36, no. 1, pp. 23-26.

812 Cuevas Gozalo, M.C. and Martinius, A.W., 1993. Outcrop database for the geological characterisation of fluvial
813 reservoirs, an example from distal fluvial fan deposits in the Loranca Basin, Spain. In: *Characterisation of*
814 *Fluvial and Aeolian Reservoirs*, Vol. 73, pp. 79–94 (eds North, C.P. and Prosser, D.J.), Special Publication
815 of the Geology Society of London.

816 Curran, P. J., 1983. *Principles of Remote Sensing*, Hong Kong, English Language Book Society (ELBS) /
817 Longman, p.1.

818 Davidson, S.K., Leleu, S. and North, C.P., 2011. *From River to Rock Record: The Preservation of Fluvial*
819 *Sediments and Their Subsequent Interpretation*, SEPM (Society for Sedimentary Geology).

820 De Rooij, M., Corbett, P. W., and Barends, L., 2002. Point bar geometry, connectivity and well test. *first break*,
821 (2012).

822 Dieras, P.L., Constantine, J.A., Hales, T.C., Piégay, H. and Riquier, J., 2013. "The role of oxbow lakes in the off-
823 channel storage of bed material along the Ain River, France", *Geomorphology*, vol. 188, no. 0, pp. 110-
824 119.

825 Doust, H., and Omatsola, E., 1990. Niger Delta, in, Edwards, J. D., and Santogrossi, P.A., eds., Divergent/passive
826 Margin Basins, AAPG Memoir 48: Tulsa, *American Association of Petroleum Geologists*, p.239-248.

827 Edmonds, D. A. and Slingerland R. L., 2007. "Mechanics of river mouth bar formation: Implications for the
828 morphodynamics of delta distributary networks." *Journal of Geophysical Research-Earth Surface* **112** (F2).

829 Edmonds, D. A. and Slingerland R. L., 2008. "Stability of delta distributary networks and their bifurcations."
830 *Water Resources Research* **44**(9).

831 Edmonds, D. A. and Slingerland R. L., 2009. Significant effect of sediment cohesion on delta morphology.
832 *Nature Geoscience*, 3(2), 105-109.

833 Egozi, R. and Ashmore, P., 2008. Defining and measuring braiding intensity. *Earth Surface Processes and*
834 *Landforms*, 33(14), pp.2121-2138.

835 Erkens, G., Cohen, K.M., Gouw, M.J., Middelkoop, H. and Hoek, W.Z., 2006. "Holocene sediment budgets of
836 the Rhine Delta (The Netherlands): a record of changing sediment delivery", *IAHS PUBLICATION*, vol.
837 306, pp. 406.

838 Erskine, W., Melville, M., Page, K. & Mowbray, P., 1982. "Cutoff and oxbow lake", *The Australian Geographer*,
839 vol. 15, no. 3, pp. 174-180.

840 Evamy, B.D., Haremboure, J., Kamerling, P., Knaap, W.A., Molloy, F.A., and Rowlands, P.H., 1978.
841 Hydrocarbon habitat of Tertiary Niger Delta: *American Association of Petroleum Geologists Bulletin*, v.
842 62, p. 277- 298.

843 Fairhead, J.D., Binks, R.M., 1991. Differential opening of the Central and South Atlantic Oceans and the
844 opening of the West African rift system. *Tectonophysics* 187, 191–203.

845 Fagan, S.D. and Nanson, G.C., 2004. "The morphology and formation of floodplain-surface channels, Cooper
846 Creek, Australia", *Geomorphology*, vol. 60, no. 1–2, pp. 107-126.

847 Ferguson, R., 1987. Hydraulic and sedimentary controls of channel pattern. In Richards, K., editor, *River*
848 *channels: environment and process*, Institute of British Geographers *Special Publication* 18, Oxford:
849 Blackwell, 129–58.

850 Fielding, C.R. and Crane, R.C., 1987. An application of statistical modelling to the prediction of hydrocarbon
851 recovery factors in fluvial reservoir sequences. In: *Recent Developments in Fluvial Sedimentology*, pp. 321–
852 327 (eds Ethridge, F.G., Flores, R.M. and Harvey, M.D.). *SEPM Special Publication* 39, Tulsa, OK.

853 Fisk, N.H., 1947. Fine-grained alluvial deposits and their effects on Mississippi River activity. Mississippi River
854 Commission Waterways Experiment Station, Vicksburg, Mississippi, p. 78

855 Friend, P.F. and Sinha, R., 1993. "Braiding and meandering parameters", *Geological Society, London, Special*
856 *Publications*, vol. 75, no. 1, pp. 105-111.

857 Giosan, L., Constantinescu, S., Clift, P.D., Tabrez, A.R., Danish, M. and Inam, A., 2006. Recent morphodynamics
858 of the Indus delta shore and shelf, *Continental Shelf Research*, vol. 26, no. 14, pp. 1668-1684.

859 Ghinassi, Massimiliano & Ielpi, Alessandro & Aldinucci, Mauro & Fustic, Milovan. (2016). Downstream-
860 migrating fluvial point bars in the rock record. *Sedimentary Geology*. 334. 10.1016/j.sedgeo.2016.01.005.

861 Giosan, L. and Goodbred Jr., S.L., 2007. FLUVIAL ENVIRONMENTS, Deltaic Environments in *Encyclopedia*
862 *of Quaternary Science*, ed. S.A. Elias, Elsevier, Oxford, pp. 704-716.

863 Grant, C. W., Goggin D. J. and Harris P. M., 1994. Outcrop analogue for cyclic-shelf reservoirs, San Andres
864 Formation of Permian Basin: stratigraphic framework, permeability distribution, geostatistics and fluid-
865 flow modeling: *American Association of Petroleum Geologist, Bulletin*, v.78, p. 23-54.

866 Guiraud, R., Maurin, J.C., 1991. Le rifting en Afrique au Cretaceinferieur: synthese structural, mise en evidence
867 de deux phases dans la genese des basins, relations avec les ouverturesoceaniquesperi-africaines. *Bull.*
868 *Soc. Geol. Fr.* 162, 811–823.

869 Guiraud, R., Maurin, J.C., 1993. Cretaceous rifting and basin inversion in Central Africa. In: Thorweihe, U.,
870 Schandelmeier, H. (Eds.), *Geoscientific Research in Northeast Africa: Rotterdam. Balkema, A. A.*, pp.
871 203–206.

872 Hill, M. B., & Webb, J. E., 1958. The ecology of Lagos Lagoon. II. The topography and physical features of
873 Lagos Harbour and Lagos Lagoon. *Philosophical Transactions of the Royal Society of London. Series B,*
874 *Biological Sciences*, 241(683), 319-333.

875 Holbrook J. and Alexandrowitz N., 2011. Rethinking the Classic Oxbow Filling Model: Some Hope for Improved
876 Reservoir Connectivity. AAPG ANNUAL CONFERENCE AND EXHIBITION *Making the Next Giant*
877 *Leap in Geosciences* April 10-13, 2011, Houston, Texas, USA.

878 Howard, A.D., 1967. Drainage analysis in geologic interpretation: a summation. *Bulletin of American Association*
879 *of Petroleum Geology*, 51, 2246-59.

880 Hoyal, D. and Sheets, B., 2009. "Morphodynamic evolution of experimental cohesive deltas", *Journal of*
881 *Geophysical Research: Earth Surface (2003–2012)*, vol. 114, no. F2.

882 Jin, Z.K., Gao B.S., Wang J.Y., Li T., Shi L., Yu K.H., and Li G.Z., 2017. Two new types of sandbars in channels
883 of the modern Ganjiang Delta, Poyang Lake, China: Depositional characteristics and origin. *Journal of*
884 *Palaeogeography*, 6(2), pp.132-143. DOI: 10.1016/j.jop.2017.03.001

885 Kelly, S. 2006. Scaling and hierarchy in braided rivers and their deposits: examples and implications for reservoir
886 modelling. In: *Braided Rivers: Process, Deposits, Ecology and Management* (Eds G.H. Sambrook-Smith,
887 J.L. Best, C.S. Bristow and G.E. Petts), *IAS Spec. Publ.*, 36, 75–106.

888 Kemp, J., 2004. Flood channel morphology of a quiet river, the Lachlan downstream from Cowra, southeastern
889 Australia. *Geomorphology*, 60(1), 171-190.

890 Kleinhans, M.G., 2010. "Sorting out river channel patterns", *Progress in Physical Geography*, vol. 34, no. 3, pp.
891 287-326.

892 Kleinhans, M.G., Cohen, K.M., Hoekstra, J. and IJmker, J.M., 2011. "Evolution of a bifurcation in a meandering
893 river with adjustable channel widths, Rhine delta apex, The Netherlands", *Earth Surface Processes and*
894 *Landforms*, vol. 36, no. 15, pp. 2011-2027.

895 Kleinhans, M. G. and van den Berg, J. H., 2011. River channel and bar pattern explained and predicted by an
896 empirical and physics-based method. *Earth Surface Processes and Landforms* 36, 721-738.

897 Komar, P.D., 1984. The Lemniscate Loopacomparisons with the shapes of streamlined landforms. *J. Geol.*, 92,
898 p. 133–145.

899 Kravtsova, V. I., Mikhailov, V. N., & Kozyukhina, A. S., 2008. Hydrological-morphological and landscape
900 features of the Niger River delta. *Water Resources*, 35(2), 121-136.

901 Kulke, H., 1995, Nigeria, In: Kulke, H., Regional Petroleum Geology of the World. Part II: Africa, American,
902 Australian and Antarctica: Berlin, Gebruder Borntraeger, p.143-172.

903 Leopold, L.P., Wolman M.G., and Miller J.P., 1964. Fluvial Processes in Geomorphology. San Fransisco, W.H.
904 Freeman & Co., 622 p.

905 Leopold, L.B. and Wolman M.G., 1960. River meanders. Geol. Soc. America Bulletin, 71, p. 769-794.

906 Luchi, R., Hooke, J.M., Zolezzi, G. and Bertoldi, W., 2010. Width variations and mid-channel bar inception in
907 meanders: River Bollin (UK). *Geomorphology*, 119(1-2), pp. 1-8.

908 Meshkova, L.V. and Carling, P.A. 2012. "The geomorphological characteristics of the Mekong River in northern
909 Cambodia: A mixed bedrock–alluvial multi-channel network", *Geomorphology*, vol. 147–148, no. 0, pp.
910 2-17.

911 Miall, A. D., 1992. Alluvial deposits, In Walker R. C. and N.P. James (eds) Facie Models: Response to sea level
912 changes, Quebec, Love Printing Service Limited, p. 121-142.

913 Nanson G, Knighton A. 1996. Anabranching rivers: their cause, character and classification. *Earth Surface
914 Processes and Landforms* 21:217–239.

915 NEDECO (Netherlands Engineering Consultants), 1954. Western Nigeria Delta, report on investigation: The
916 Hague, p. 143.

917 NEDECO (Netherlands Engineering Consultants), 1959. River studies and recommendations on improvement of
918 Niger-Benue Rivers, North Holland Publishing Co. p.1000.

919 NEDECO, (Netherlands Engineering Consultants), 1961. The waters of Niger Delta: The Hague, p. 317.

920 Nichols, G., 1999. *Sedimentology and Stratigraphy*, London, Blackwell science limited, p. 118.

921 North, C. P., 1996. The prediction and modelling of subsurface fluvial stratigraphy. In P. A. Carling and M. R.
922 Dawson (eds), *Advance in Fluvial Dynamics and stratigraphy*. New York: John Wiley and Sons Ltd, p.
923 396-508.

924 Olade, M.A., 1975. Evolution of Nigeria’s Benue Trough (Aulacogen): a tectonic model. Geol. Mag. 112 (6),
925 575–583.

926 Olariu, C., and Bhattacharya, J. P., 2006. Terminal distributary channels and delta front architecture of river-
927 dominated delta systems. *Journal of Sedimentary Research*, 76(2), 212-233.

928 Oomkens, E., 1974. Lithofacies relations in late quaternary Niger Delta Complex, *sedimentology*, volume: 21,
929 Issue: 2 p. 195-222

930 Parker, G. and Sequeiros, O., 2006. "Large scale river morphodynamics: Application to the Mississippi Delta",
931 *River Flow 2006: Proceedings of the International Conference on Fluvial Hydraulics, Lisbon, Portugal,
932 6–8 September 2006*, pp. 3

933 Pierik, H.J., Stouthamer E. and Cohen K.M., 2017. Natural levee evolution in the Rhine-Meuse delta, the
934 Netherlands, during the first millennium CE. *Geomorphology*, 295, pp.215-234. DOI:
935 10.1016/j.geomorph.2017.07.003

936 Reading, H. G. (ed.) 1996, *Sedimentary Environments: Processes, Facies and Stratigraphy*, 3rd ed. Oxford:
937 Blackwell, 688 pp.

938 Reijer, T. J. A., 1996, *Selected Chapter on Geology: Sedimentary Geology and Sequence Stratigraphy in Nigeria
939 and three case studies as a Field Guide*, Warri, SPDC Corporate Reprographics.

940 Roberts H.H., Weimer P., and Slatt R. M., 2012. River deltas: In Roberts D.G and Bally A. W. (ed), 2012.
941 *Regional Geology and Tectonics: Principles of Geologic Analysis*, Elsevier, Pages 490-511.

942 Sambrook Smith, G.H., Ashworth, P.J., Best, J.L., Woodward, J. and Simpson, C.J., 2005. The morphology and
943 facies of sandy braided rivers: some considerations of scale invariance. *Fluvial sedimentology VII*, pp.145-
944 158.

945 Sarg, J. F., Markello J. R., and Weber L. J., 1999. The second order cycle, carbonate-platform growth. And
946 reservoir, source, and trap prediction, in P.M. Harris, A. H. Saller, and J. A. Simo, eds., *Advances in*
947 *carbonate sequence stratigraphy: Application to reservoirs, outcrop, and model: SEPM Special Publication*
948 63, p. 11-31.

949 Schumm, S. A., 2005. *River variability and complexity*. Cambridge University Press.

950 Schumm, S.A., Dumont, J.F., and Holbrook, J.M., 2000. *Active Tectonics and Alluvial Rivers*: Cambridge, U.K.,
951 Cambridge University Press, p. 276.

952 Seppälä, M., 2013. River sinuosity measured by the Mansikkaniemi method: a critical evaluation. *Fennia-*
953 *International Journal of Geography*, 161(2), 303-310.

954 Short, K.C. and Stauble A. J., 1967. Outline of the Geology of the Niger Delta, *American Association of Petroleum*
955 *Geologist, Bulletin*, v. 51, p. 761-779.

956 Spagnolo, M.; Llopis, I.A.; Pappalardo, M., and Federici, P.R., 2008. A new approach for the study of the coast
957 indentation index. *Journal of Coastal Research*, 24(6), pp1459–1468.

958 Strahler, A. N., 1957. Quantitative analysis of watershed geomorphology. *Civ. Eng*, 101, 1258-1262.

959 Stokes M and Mather AE., 2003. Tectonic origin and evolution of a transverse drainage: the Rio Almanzora, Betic
960 Cordillera, Southeast Spain' *Geomorphology* 50 (1-3), pp 59 - 81

961 Stoneley, R., 1965. The Niger Delta region in the light of the theory of Continental Drift: *Geol. Magazine*, vol
962 103, p. 385-396.

963 Tuttle, M. L., Charpentier, R. R., and Brownfield, M. E., 1999, *The Niger Delta Petroleum System: Niger Delta*
964 *Province, Nigeria, Cameroon, and Equatorial Guinea, Africa*. US Department of the Interior, US
965 Geological Survey.

966 Tyler, N., and Finley, R.J., 1991. Architectural controls on the recovery of hydrocarbons from sandstone
967 reservoirs, in Miall, A.D., and Tyler, N., eds., *The Three-dimensional Facies Architecture of Terrigenous*
968 *Clastic Sediments, and Its Implications for Hydrocarbon Discovery and Recovery: SEPM, Concepts and*
969 *Models in Sedimentology and Paleontology*, no. 3, p. 1–5.

970 Uehlinger, U., Wantzen, K.M., Leuven, R.S.E.W. and Arndt, H., 2009. Chapter 6 - The Rhine River Basin. *Rivers*
971 *of Europe*. London: Academic Press, pp. 199-245.

972 Vakarelov, B. K., & Ainsworth, R. B., 2013. A hierarchical approach to architectural classification in marginal-
973 marine systems: Bridging the gap between sedimentology and sequence stratigraphy, *Hierarchical*
974 *Marginal-Marine Architectural Classification*. *AAPG Bulletin*, 97(7), 1121-1161.

975 Van Balen, R. T., Busschers, F. S., and Tucker, G. E., 2010. Modeling the response of the Rhine–Meuse fluvial
976 system to Late Pleistocene climate change. *Geomorphology*, 114(3), 440-452.

977 White, C. D., and Barton, M. D., 1999. Translating Outcrop Data to Flow Models, with Applications to the Ferron
978 Sandstone. *SPE Reservoir Evaluation & Engineering*, 2(04), 341-350.

979 White, J. Q., Pasternack, G. B., and Moir, H. J., 2010. Valley width variation influences riffle–pool location and
980 persistence on a rapidly incising gravel-bed river. *Geomorphology*, 121(3), 206-221. Whiteman A., 1982,
981 *Nigeria: Its Petroleum Geology Resources and Potentials*, London, Graham and Trotman Limited, volume
982 1, p. 110-166.

983 Whiteman A., 1982, *Nigeria: Its Petroleum Geology Resources and Potentials*, London, Graham and Trotman
984 Limited, volume 1, p. 110-166.

985 Willis, B.J. and Gabel, S. 2001." Sharp-based, tide-dominated deltas of the Sego Sandstone, Book Cliffs, Utah,
986 USA", *Sedimentology*, vol. 48, no. 3, pp. 479-506.

987 Wood, L. J., 2004. Quantitative Seismic Geomorphology of Clastic Reservoirs and Systems. Houston Geological
988 Society Bulletin, Volume 47, No. 4, December 2004. Pages 19-21, 23-25, 47(4), 19-21, 23-25.

989 Woodrofe, C. D. 2000. Deltaic and estuarine environments and their late Quaternary dynamics on the Sunda and
990 Sahul shelves. *Journal of Asian Earth Sciences* 18:393–413.

991 Xue, Z., Liu, J. P., DeMaster, D., Van Nguyen, L., and Ta, T. K. O., 2010. Late Holocene evolution of the Mekong
992 subaqueous delta, southern Vietnam. *Marine Geology*, 269(1), 46-60.

993 Zimmermann, J., Franz M., Schaller A. and Wolfgramm M., 2018. The Toarcian–Bajocian deltaic system in the
994 North German Basin: Subsurface mapping of ancient deltas-morphology, evolution and controls.
995 *Sedimentology*, 65(3), pp.897-930. DOI: 10.1111/sed.12410